PHYSICAL REVIEW LETTERS

VOLUME 5 DECEMBER 1, 1960 NUMBER 11

ION RESONANCE IN A MULTICOMPONENT PLASMA

S. J. Buchsbaum
Bell Telephone Laboratories, Murray Hill, New Jersey

(Received October 19, 1960)

We have performed experiments designed to study the phenomena associated with ion cyclotron resonance in a multicomponent plasma whose charged particle density is sufficiently high that interaction between the various plasma components takes place. We present here a preliminary account of the experimental results.

The transverse oscillations of a uniform, cold plasma in an axial, uniform magnetic field have been studied by a number of authors.[1-4] In Fig. 1 are shown the resonant frequencies of a hydrogen plasma which, for the sake of an example, is assumed to contain the ions H_1^+, H_2^+, and H_3^+ in relative concentrations of 5%, 50%, and 45%, respectively. These frequencies were calculated[3,4] assuming no collisions by finding the roots of the equation $k_x(\omega)=\infty$, where k_x is the propagation constant of an extraordinary wave propagating at right angles to the magnetic field. Equations (2) and (7) of reference 4 are examples of the results of such calculations. The curve marked A in Fig. 1 is given by

$$\omega^2=\omega_b^2+\omega_p^2, \qquad (1)$$

where $\omega_b=eB/m$ is the electron cyclotron frequency and $\omega_p=(ne^2/m\epsilon_0)^{1/2}$ is the electron plasma frequency. This resonance (included for completeness) is of no concern in this experiment as it occurs at microwave frequencies and depends only upon the motions of electrons. Curves B, C, and D are associated with ion motions and are of interest here. At low plasma densities ("low" to be defined shortly), where sufficient space-charge field to couple the motions of the various plasma components cannot be induced in the plasma, resonance is at the cyclotron frequencies of each ion species. At high plasma densities, curve B tends to the so-called electron-ion hybrid frequency. This limit was studied by Auer et al.[2] and in great detail by Körper,[3] who showed that for a plasma with a single ion species it is given

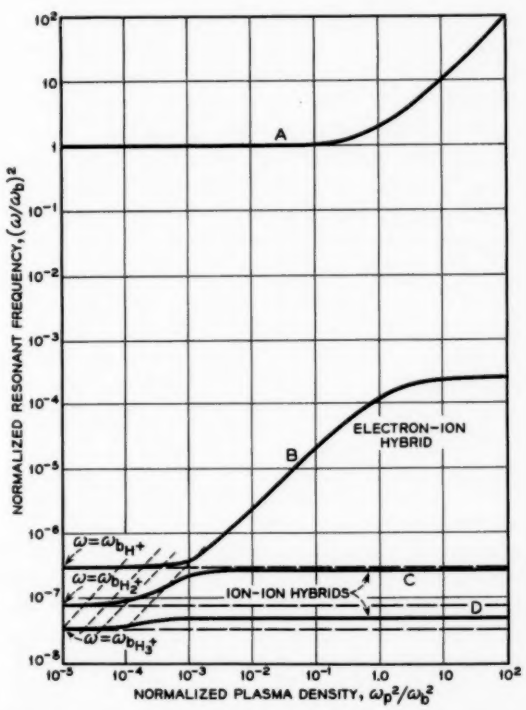

FIG. 1. Calculated resonant frequency of a hydrogen plasma as a function of plasma density and magnetic field. The following ions are assumed present in the indicated concentration: H^+(5%), H_2^+(50%), and H_3^+(45%).

by

$$\omega^2 = \omega_b \omega_{bi}, \tag{2}$$

where $\omega_{bi} = eB/M_i$ is the ion cyclotron frequency. For a many-component plasma ω_{bi} must be replaced by $\sum_i x_i \omega_{bi}$, where x_i is the relative concentration of the ith ion species. Curves C and D tend to the so-called ion-ion hybrids. It was shown in reference 4 in a three-component plasma that at these resonances the various ion species oscillate out of phase with each other while the electrons remain relatively motionless. The ion-ion hybrid frequencies are then sensibly independent of the electron cyclotron frequency and depend only on ion cyclotron frequencies and on the relative concentrations of the different ion species. For a plasma with more than two ions this dependence is sufficiently involved that the discussion of it must be postponed to a more detailed publication.[5] Here it suffices to say that the solid curves in Fig. 1 never cross the horizontal dashed ones, and that the larger the relative concentration of a particular ion species the closer does its hybrid frequency approach the cyclotron frequency of the next lighter ion. Of importance in these experiments are the "knees" in curves B, C, and D at low plasma densities. They mark the transition from a single-particle behavior to a collective one; "pure" ion cyclotron resonance occurs in the region to the left of the knee. The density at which a knee occurs depends on concentrations of all ions,[5] but pure ion cyclotron resonance generally obtains provided

$$\omega_p^2 \ll \omega_b \omega_{bi}, \tag{3}$$

where ω_{bi} is the cyclotron frequency of the ion in question. Ion-ion hybrids are attained at densities such that the inequality (3) is reversed, while for the electron ion hybrid one must have $\omega_p^2 \gg \omega_b^2$.

The aim of the experiment was to observe "pure" ion cyclotron resonance and to study the behavior of the resonance with increasing plasma densities. The experiment was performed on the positive column of an arc discharge with a thermionically heated oxide-coated cathode. The tube was connected to a vacuum system, which could be baked out and which could be filled with gas to any desired pressure. The gas used was "spectroscopically pure" hydrogen, helium, or neon provided by the Linde Company. Some, but not great, attention was paid to maintaining the gas purity. The positive column was in an axial magnetic field provided by a Bitter-type solenoid. The large magnetic field (up to 85 kgauss) enables one to perform the experiment at elevated frequencies (6.2, 10.8, 18.18, and 27.3 Mc/sec were used) with a corresponding decrease in linewidths. Also, as (3) reduces to $n \ll [6\times10^7 (B \text{ kgauss})^2/(M_i \text{ atomic units})]$ cm^{-3}, "pure" cyclotron resonance can be observed at densities which can be obtained in active gas discharges. The central portion of the positive column was surrounded by a resonant structure which, in the absence of a plasma, produced a "twisted" electric potential given by

$$\varphi(r,\theta,z) = \varphi_0 I_m(k_z r)\cos(m\theta \pm k_z z)\cos\omega t; \quad m = 1, 2 \tag{4}$$

where I_m is the modified Bessel function. The presence of the plasma modifies the argument of I_m which then exhibits the resonances shown in Fig. 1. The twist in the electric potential makes it possible for the rf field to penetrate the plasma more completely,[6] and is given by the axial wave number k_z ($k_z \gg \omega/c$). The static magnetic field was uniform to within 4% over the interaction region. The absorption and dispersion were measured at a constant tube current and a constant gas pressure as a function of the magnetic field by measuring on an rf bridge the changes in the effective admittance of the resonance structure caused by the plasma. This corresponds to motion along the diagonal lines in Fig. 1. No substantial change in the absorption lines was found experimentally when the dipole field [$m = 1$ in Eq. (4)] was replaced by the quadrupole field ($m = 2$).

Figure 2 is an example of "pure" or almost pure ion cyclotron absorption lines in helium with a hydrogen impurity. In Fig. 2(a) the H^+ and H_2^+ lines are at their cyclotron fields while the H_3^+ line is slightly shifted toward lower magnetic field, i.e., toward its hybrid field. There is also evidence for a shifted He^+ line. Figure 2(b) is a dispersion curve.

In Fig. 3 we plot the absorption in relatively pure hydrogen for various plasma densities. At the lowest plasma densities ($I_p = 2.6$ ma) at which the signal-to-noise ratio allowed a reproducible run, the H_3^+ line is at its cyclotron field and the H_2^+ and H^+ lines are broad and already shifted towards lower B fields. As the plasma density increases, all three lines shift towards lower fields in qualitative agreement with Fig. 1. The shift from cyclotron resonance to hybrid resonance requires an increase in density of approximately two orders of magnitude, in agreement

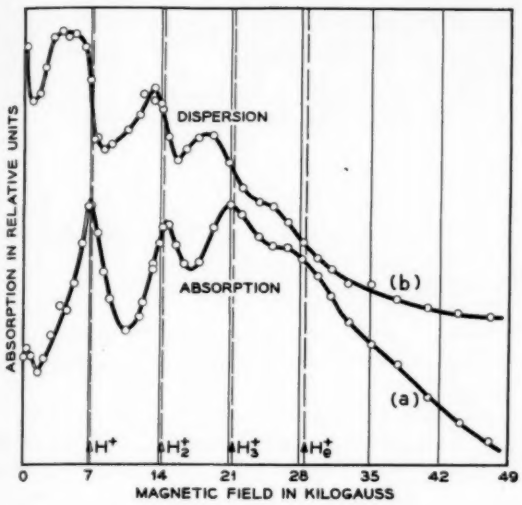

FIG. 2. Absorption and dispersion in a helium plasma with hydrogen impurity. Helium pressure = 100 microns; hydrogen concentration unknown but less than 2%. Quadrupole field, $f = 10.82$ Mc/sec. Tube current = 8 ma. The arrows indicate the cyclotron fields of the various ions.

with Fig. 1. A quantitative comparison with theory cannot yet be made. We do not know the relative concentrations of the various ions in the plasma which, moreover, are apt to vary as the plasma density is increased. There exists, however, one notable disagreement with Fig. 1. The H_3^+ line definitely crosses the H_2^+ cyclotron field and the H_2^+ line crosses the H^+ field. The reason for this is not yet known, but it is thought to result from the presence of density gradients in the plasma. The behavior of linewidths with increasing density is of interest. The width of the H_3^+ line increases, while that of the H_2^+ line decreases. This is reasonable, however, for the following reasons. In the transition region between cyclotron and hybrid resonances, the frequency (and thus the resonant magnetic field) is density dependent. In a nonuniform plasma one then expects the line to be additionally broadened. Now, in Fig. 3 the H_3^+ line is in the low-density part of the transition region, while the H_2^+ line is in the high-density part of it; it is this fact which, it is now thought, may account for the apparently anomalous behavior of the linewidths.

Results similar to, but not identical with, those shown in Fig. 3 were obtained at other frequencies and pressures and for various other gases.[5]

The author is grateful to H. W. Dail, N. R. Sheeley, and A. S. Wilczek whose aid made this experiment possible. Many stimulating discussions with J. K. Galt are acknowledged.

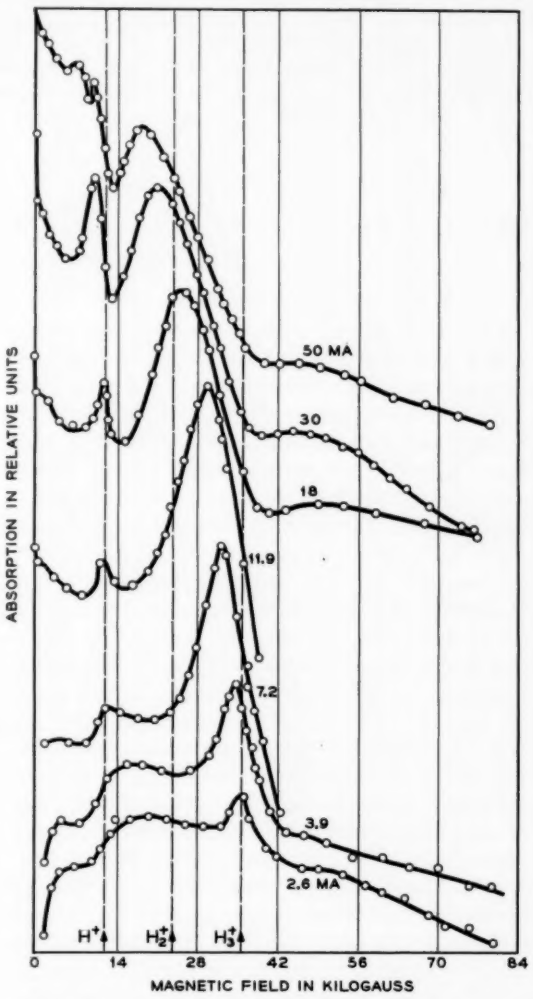

FIG. 3. Absorption in a hydrogen plasma for various plasma densities (tube currents), pressure = 110 microns. Dipole field, $f = 18.18$ Mc/sec. The arrows indicate the cyclotron fields of the various ions. The origin of the structure in the absorption lines at high magnetic fields is not known.

[1]E. Astrom, Arkiv Fysik 2, 443 (1950).
[2]P. L. Auer, H. Hurwitz, Jr., and R. D. Miller, Phys. Fluids 1, 501 (1958).
[3]K. Körper, Z. Naturforsch. a12, 815 (1957); a12, 220 (1960).
[4]S. J. Buchsbaum, Phys. Fluids 3, 418 (1960).
[5]S. J. Buchsbaum (to be published).
[6]T. H. Stix, Phys. Rev. 106, 1146 (1957); T. H. Stix and R. W. Palladino, Phys. Fluids 1, 446 (1958).

CONTRIBUTION OF THE FERMI CONTACT TERM TO THE MAGNETIC FIELD AT THE NUCLEUS IN FERROMAGNETS*

A. J. Freeman,
Materials Research Laboratory, Ordnance Materials Research Office, Watertown, Massachusetts and Solid State and Molecular Theory Group, Massachusetts Institute of Technology, Cambridge, Massachusetts

and

R. E. Watson,†
AVCO, RAD, Wilmington, Massachusetts and Solid State and Molecular Theory Group, Massachusetts Institute of Technology, Cambridge, Massachusetts

(Received November 10, 1960)

Recent Mössbauer measurements[1] have revealed a large but unexpectedly[2] negative (-333 kgauss) effective magnetic field, H_e, at the Fe^{57} nucleus in ferromagnetic iron. These results led to the recognition[1] that the dominant source of H_e must come from the polarization of the core s electrons which then contribute a field, H_c, through the Fermi contact interaction. We are here reporting results for a set of calculations[3] for H_c which are based on a model consistent with neutron diffraction[4] and energy band results.[5] These results are compared with those just reported by Goodings and Heine[6] for a less realistic model. Both calculations are shown to be deficient in that the experimental value of H_e is not realized, and hence that the dominance of the core contribution has not been proven. Some striking results are also reported for an investigation of H_c as a function of the position of the $3d$ density in the atom. These results help to clarify the theoretical picture and should lead to a proper theoretical treatment of the problem.

Our investigations are based on "spin (exchange) polarized" Hartree-Fock[3] calculations, i.e., calculations in which electrons in the same shell, but differing in spin direction (m_s) are allowed different radial distributions. Physically, this difference arises, in atoms having a net spin, from the different exchange interactions experienced by electrons of majority (say up, ↑) and minority (↓) spins. The resultant difference in radial distributions leads to a difference in density for s electrons at the nucleus, $|\psi_\uparrow(0)|^2 - |\psi_\downarrow(0)|^2$, which contributes to H_e through the Fermi contact interaction. A convenient measure of this interaction is given by

$$\chi = (4\pi/S)\sum_{\text{shells}}\{|\psi_\uparrow(0)|^2 - |\psi_\downarrow(0)|^2\},$$

where S designates the number of unpaired electrons. For divalent transition element ions, experimental values of χ are known[7] to be roughly constant (~ -3 atomic units) and this has led to the general assumption of spin polarization effects linear in total spin.

We have calculated χ for the free ions Mn^{+2}, Fe^{+2}, and Ni^{+2}; the resulting χ's are -3.34, -3.29, and -3.94 a.u., respectively. We also obtained a χ of -3.27 a.u. for Ni^{+2} in a crude (i.e., point charge) crystalline field. The variation in χ for the Ni^{+2} calculations is due to its extreme sensitivity to the behavior of the $3d$ spin distribution. The calculated χ's are consistently more negative than experimental values and this overestimation appears to be a general result of such calculations.[1]

Marshall's[2] estimates for the outer electrons in metallic Co gave a contribution to the magnetic field of about +260 kgauss. Such estimates are necessarily crude, but probably 200 kgauss for these terms in Fe is reasonable. (Goodings and Heine estimated this to be between +120 and +300 kgauss.) To give a net H_e of -333 kgauss in Fe^{57}, the actual H_c must be ~-530 kgauss (or there must be another, as yet uninvestigated negative contribution). If we estimate by assuming, as for the divalent ions, that χ is about -3 a.u., then H_c for the metal core (with 2.2 unpaired spins) is only -280 kgauss and this is clearly not enough.

To account for this large difference between core polarizations in metals and ions, several factors were considered. It is generally assumed that in metallic iron there are between 7 and 8 electrons in the $3d$ band (as against 6 for the neutral atom or divalent ion). Furthermore, theoretical evidence[5] indicates that the $3d$ electrons in the metal are more expanded than in the free ($3d^6 4s^2$) atom. We have therefore done a full Hartree-Fock spin (exchange) polarized calculation for Fe in both $3d^6 4s^2$ and $3d^6$ configurations. As shown in Fig. 1, even though the $3d^6$ one-electron $3d$ charge density is expanded relative to the $3d^6 4s^2$, the resultant one-electron $3d$ spin density (the relevant factor determining H_c)[3] is not significantly changed. This spin density agrees with

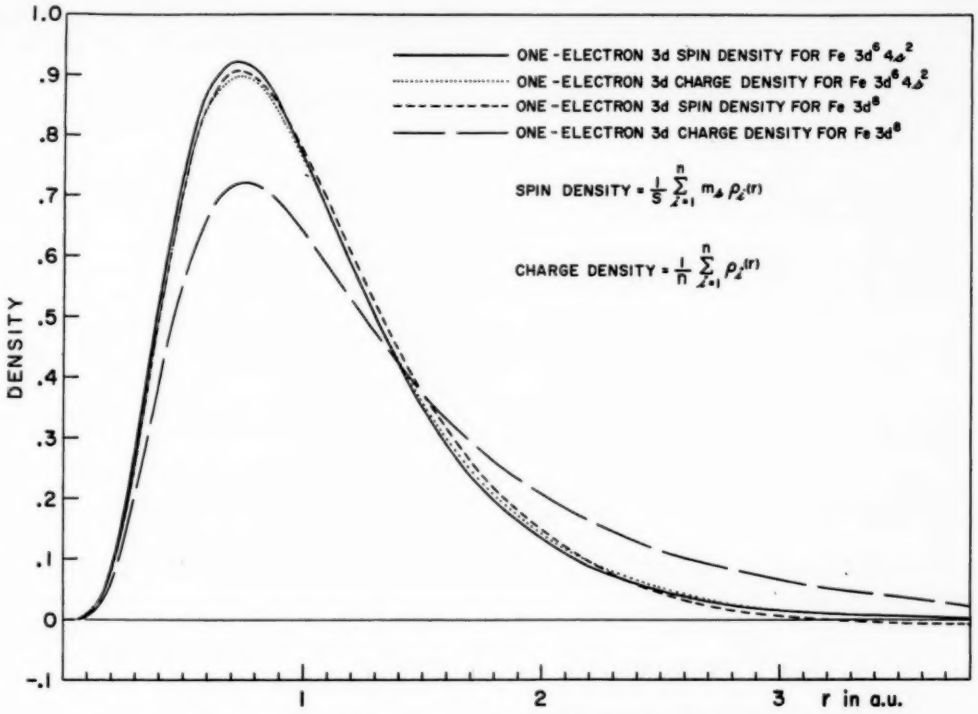

FIG. 1. One-electron $3d$ spin and charge densities for Fe $3d^6 4s^2$ and $3d^8$.

neutron measurements[4] and energy band calculations[5] which give a spin density which is actually slightly contracted relative to the free $3d^6 4s^2$ atom. For Ni^{+2}, such a contraction in spin density was shown to reduce H_c.[3]

For the $3d^8$ state, the calculated H_c (-350 kgauss) is 30 kgauss lower than the $3d^6 4s^2$ value (both are overestimated by about 40 kgauss). This improvement is too small to overcome the positive contributions and so cannot account for the experimental result.

Goodings and Heine[6] did a $3d^6 4s^2$ free-atom spin polarized calculation for Fe and obtained a χ of -3.8 a.u. (-355 kgauss) from the core. The difference between this value and our own arises from the computational sensitivity of the calculations (thus the best one can hope to do is to provide a consistent set of computations). Their χ (and ours) shows the overestimation discussed above. To estimate the effect in a metal, they repeated the calculation with fixed "$3d$ functions artificially expanded by about 5% at the maxima and 10% over the tail regions." This lowered H_c (by 65 kgauss) to -420 kgauss. This, they felt, sufficiently balanced the positive contribution at their lower limit (+120 kgauss) to make the calculated H_c explain the experimental H_e.

We do not agree. If their free-atom overestimate of H_c is corrected (from -355 to ~ -280 kgauss), then their expanded $3d$ value of H_c would be changed from -420 kgauss approximately back to their quoted free-atom value. Furthermore, their "artificial $3d$ expansion" gives a spin density in direct disagreement with the neutron diffraction and energy band results cited above.

An investigation of H_c as a function of the position of the $3d$ density in the atom helps to clarify the theoretical picture. For a series of fixed $3d$ functions (which for computational simplicity we took as a single Slater atomic orbital), we determined H_c via spin-polarized Hartree-Fock calculations. The results are shown in Fig. 2 as a function of the maxima of the $3d$ orbitals.

We see that a large, but unrealistic, expansion or contraction of the $3d$ shell spin density will yield an H_c which is more than sufficient to "explain" the metal results. Simple scaling does not appear to be the answer to the problem.[9] On the other hand, Fig. 2 suggests that any (other) ad hoc small change of shape in the $3d$ functions

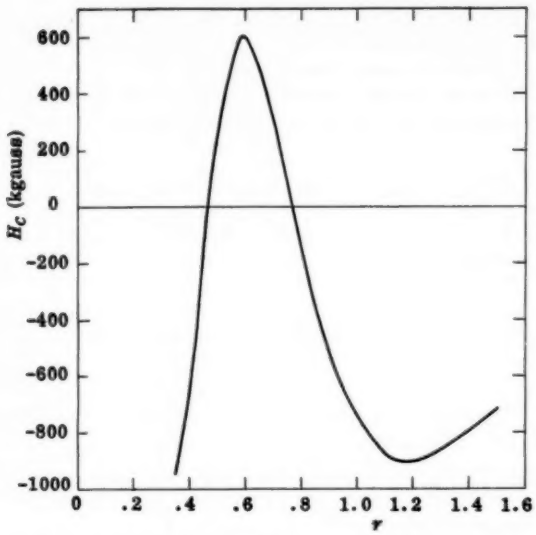

FIG. 2. Core effective field, H_C, as a function of the maximum of the 3*d* orbital for Fe $3d^8$.

which removes spin density from the region roughly between 0.5 and 0.75 a.u. will yield a substantial lowering of H_C. This can be devised while maintaining reasonable compatibility with the neutron measurements.

What is needed is a theoretical treatment which gives a more realistic description of the atom's environment, the importance of which is indicated by the experimental results[10] for Fe^{57} in Fe, Co, and Ni.

We are indebted to W. Marshall, R. K. Nesbet, and R. J. Harrison for valuable discussions and assistance.

*Some of the material in this Letter was discussed at the Sixth Conference on Magnetism and Magnetic Materials, November 14-17, New York City, Suppl. J. Appl. Phys. (to be published).

†The work of this author has been supported in part by the Ordnance Materials Research Office.

[1]S. S. Hanna, J. Heberle, G. J. Perlow, R. S. Preston, and D. H. Vincent, Phys. Rev. Letters 4, 513 (1960).

[2]W. Marshall, Phys. Rev. 110, 1280 (1958).

[3]Calculations for Ni^{+2} and details of the formalism appear in R. E. Watson and A. J. Freeman, Phys. Rev. 120, 1125, 1134 (1960).

[4]R. Nathans, C. G. Shull, A. Andreson, and G. Shirane, J. Phys. Chem. Solids 10, 138 (1959); R. J. Weiss and A. J. Freeman, J. Phys. Chem. Solids 10, 147 (1959).

[5]J. H. Wood, Phys. Rev. 117, 714 (1960).

[6]D. A. Goodings and V. Heine, Phys. Rev. Letters 5, 370 (1960).

[7]A. Abragam, J. Horowitz, and M. H. L. Pryce, Proc. Roy. Soc. (London) A230, 169 (1955).

[8]This is in large part due to lack of symmetrization, i.e., the total wave function is not, but should be, an eigenfunction of S^2.

[9]It is apparently always the case that shape and not scaling is the important feature.[3]

[10]See a recent review by G. K. Wertheim, Suppl. J. Appl. Phys. (to be published).

OPTICAL ACTIVITY IN TELLURIUM

K. C. Nomura
Honeywell Research Center, Hopkins, Minnesota
(Received October 21, 1960)

The crystal structure[1] of the elemental semiconductor, tellurium, has a symmetry which places it in an enantiomorphous class. Since this kind of symmetry constitutes only a necessary condition for the existence of optical activity, this effect was examined in single crystals and tellurium was found to have a large rotatory power. Thus, this is the first of the space-group-dependent properties to be measured in this semiconductor.

Both left- and right-handed single crystals were grown by the Czochralski method[2] which correspond to the space groups D_3^6 and D_3^4, respectively. Such crystals are levo- and dextrorotatory. At the initial stages of this work, all of our crystals were found to be dextrorotatory. This, of course, was to be expected since all of our crystals were "descended" from the same parent seed of a few years ago. The levorotatory crystals were grown from seeds which were randomly grown as needles in a hydrogen atmosphere. We would reasonably expect that such needles would have equal likelihood of being left- or right-handed. Quite fortuitously, a levorotatory crystal was grown on the second attempt.

The samples were cut into thicknesses varying

from 0.212 cm to 1.12 cm with plane parallel faces on the (0001) plane. The faces were lapped, polished in chromic acid, and oriented on (0001) with an accuracy of better than 0.5 degree. The latter is particularly important to prevent spurious interference effects.[3] The measurements were made using a Perkin-Elmer, Model 112, single-beam double-pass infrared spectrometer with NaCl optics. Stacked plates of AgCl were used for polarizers, and advantage was taken of the inherent 30% instrument polarization by placing the second polarizer in the same polarization orientation. A well-collimated plane polarized beam was directed normal to the first face of the crystal, and the sample was rotated to insure that misorientations and misalignment effects were not present. This general procedure was found to give results which were in agreement with the published values[4] for natural single crystals of α quartz.

It is conventional in optical activity experiments to express the specific rotatory power (θ/d) (quoted in units of degrees of rotation per mm of sample thickness) as a function of wavelength or wave number. The results for both levo- and dextrorotatory crystals are shown in Fig. 1, in which the abscissa is expressed in terms of the wave number $\tilde{\nu}$ (in cm^{-1}) so that deviation from normal rotatory dispersion can be seen.

These results may now be analyzed in terms of Fresnel's expression for the specific rotatory power:

$$\theta/d = 18(n_R - n_L)\tilde{\nu}, \quad \text{(degrees/mm)}$$

where $\tilde{\nu}$ is in cm^{-1}. The quantity, $n_R - n_L$, is the difference in refractive indices for the ordinary and extraordinary rays in the direction of the optic axis. At $\tilde{\nu} = 0.20 \times 10^4\ \mathrm{cm}^{-1}$ (5 microns), $n_R - n_L = \pm 1.58 \times 10^{-3}$, values some fifty times greater than for α quartz at $\lambda = 0.589$ micron.

From the curves of Fig. 1, it is seen that deviations from normal dispersion occur for $\tilde{\nu} > 0.20 \times 10^4\ \mathrm{cm}^{-1}$. This is consistent with refractive index results reported by Hartig and Loferski[5] and by Caldwell and Fan.[6]

It is a pleasure to thank L. P. Beardsley for his capable assistance, A. Ryberg who grew the crystals, and J. S. Blakemore for many useful discussions.

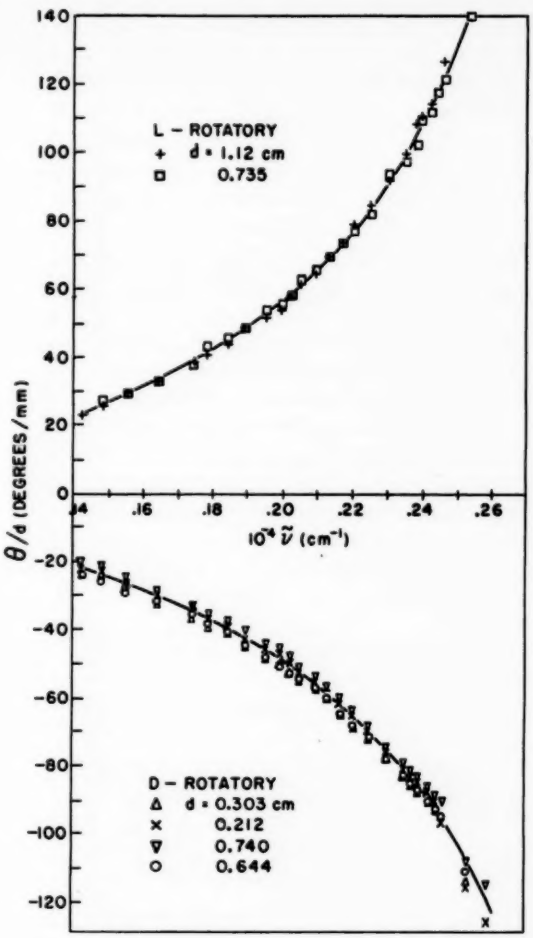

FIG. 1. The rotatory powers of dexro- and levorotatory tellurium as a function of wave number.

[1]J. J. Loferski, Phys. Rev. 93, 707 (1954).
[2]T. J. Davies, J. Appl. Phys. 28, 1217 (1957).
[3]M. Born and E. Wolf, Principles of Optics (Pergamon Press, New York, 1959), p. 695.
[4]W. E. Forsythe, Smithsonian Physical Tables, (Smithsonian Institution, Washington, D. C., 1954), 9th rev. ed., p. 558.
[5]P. A. Hartig and J. J. Loferski, J. Opt. Soc. Am. 44, 17 (1954).
[6]R. S. Caldwell and H. Y. Fan, Phys. Rev. 114, 664 (1959).

ROOM-TEMPERATURE DISLOCATION DECORATION INSIDE LARGE CRYSTALS*

Charles B. Childs
National Aeronautics and Space Administration, Goddard Space Flight Center, Greenbelt, Maryland
and
Lawrence Slifkin
University of North Carolina, Chapel Hill, North Carolina
(Received November 8, 1960)

The usual techniques for decoration of dislocations in ionic crystals[1] generally either require a high-temperature annealing treatment or else display only those dislocations near the crystal surface. For the study of some aspects of the plasticity of ionic crystals, it would be desirable to have a means of observing dislocation configurations throughout large regions of the interior of the specimen without the necessity of an annealing procedure which also changes the dislocation arrays. This note describes such a technique which displays with great contrast the distribution in the interior of large single crystals of silver chloride.

The work of Castle[2] has demonstrated that if internal print-out silver is deposited within the crystal by means of sweeping in surface-produced photoelectrons (the Haynes-Shockley method), one can see something of the dislocation structure of the crystal. Since direct observation was presumably difficult because of the excessive amount of light scattered by random, submicroscopic silver specks, Castle sectioned his specimen and looked at the microscopic silver precipitates revealed on each freshly cut surface. This method thus did not yield the large-region views produced by the precipitation processes of Amelinckx[1] and of Mitchell and co-workers.[1]

The essential contribution of the present note is the discovery that, after production of only moderate print-out densities by means of the Haynes-Shockley method, a room temperature aging of the crystal results in extensive migration of silver from random submicroscopic specks into the dislocations. After a period of several days the dislocations have become so sharply decorated relative to the diffuse background that they may be plainly observed even with ordinary bright field microscopy and a simple 20× objective, the working distance of which is great enough to allow of continuous examination deep into the crystal. In addition to random dislocations, structures such as pure tilt boundaries, square and hexagonal nets, and helices have been observed. The accompanying photographs (Figs. 1 and 2) illustrate the resolution and clear contrast achieved. The five specimens employed were Harshaw crystals which had previously been annealed in air on quartz powder.

It appears, then, that whereas the electron traps of greatest total cross section inside the crystal are not dislocations (perhaps they are impurity atoms), the most stable sites for the final precipitated silver are largely at dislocations. The migration of silver is most probably as ions plus electrons. Suptitz[3] has shown that the rate of this migration is greatly enhanced by

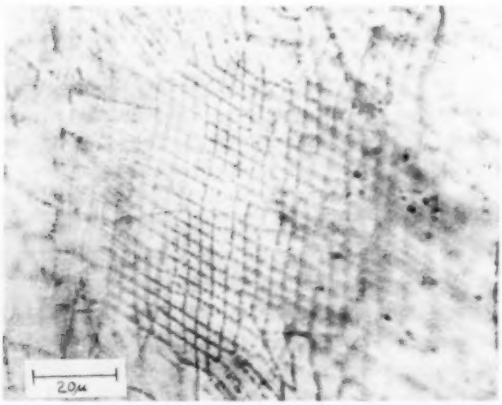

FIG. 1. A square net of dislocations.

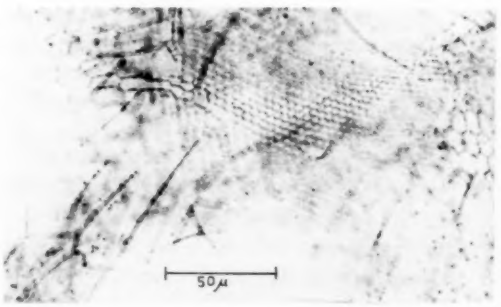

FIG. 2. A hexagonal net of dislocations.

irradiation of the crystal with visible light, presumably a photoionization effect. This suggests the possibility of accelerating the decoration process by long-wavelength irradiation. It would also appear that any effect of internal print-out on the plastic yield stress of silver chloride crystals would initially be relatively small, but would increase greatly as the silver migrated to the dislocations. Miller,[4] in this laboratory, has indeed found that the initial hardening is only slight; experiments are now under way to investigate the effects of aging.

Among the experiments suggested by this decoration technique are studies of possible internal dislocation sources and stress-induced pileups in silver chloride. Since any slow room temperature recovery is expected to be arrested at an early stage in the decoration process, it should be possible to study the dislocation distributions resulting from plastic deformation without the necessity of an intervening opportunity for their rearrangement.

*This research was performed at the University of North Carolina. The support of the University Research Council and the Air Force Office of Scientific Research is gratefully acknowledged.

[1]See, for example, J. T. Bartlett and J. W. Mitchell, Phil. Mag. 5, 445 (1960); and S. Amelinckx, Phil. Mag. 3, 307 (1958).

[2]J. W. Castle, J. Appl. Phys. 28, 743 (1957).

[3]P. Suptitz, Z. wiss. Photographie 53, 201 (1959).

[4]M. Miller (to be published).

ELECTRONIC CONDUCTION AND EXCHANGE INTERACTION IN A NEW CLASS OF CONDUCTIVE ORGANIC SOLIDS

R. G. Kepler, P. E. Bierstedt, and R. E. Merrifield
Central Research Department, Experimental Station,
E. I. du Pont de Nemours and Company, Wilmington, Delaware
(Received November 7, 1960)

A group of highly conductive organic solids which offer a unique opportunity for experimental study of electronic conduction and interaction in solids has recently been discovered in this laboratory. These materials are salts of the radical-anion formed by addition of an electron to tetracyanoquinodimethan (TCNQ):

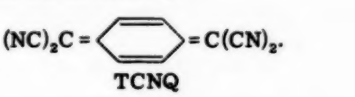

TCNQ

In combination with a variety of cations, the $[TCNQ\cdot]^-$ radical-anion forms two series of salts having the compositions

$$M^+[TCNQ\cdot]^- \text{ and } M^+[TCNQ\cdot]^-[TCNQ]^0,$$

respectively.[1] In both types of salt the band formed from the lowest normally unfilled molecular orbital of the TCNQ is partially filled, being half filled for the first series of salts and one-quarter filled for the second. As a result of the relatively weak intermolecular interactions characteristic of molecular crystals, this band will be quite narrow. In addition, both the bandwidth and the exchange coupling of the odd electrons[2] appear to be strongly influenced by the nature of the cation M^+, and by whether or not $[TCNQ]^0$ is present in the crystal.

In the quinolinium salt (see Table I), the electrons of the $[TCNQ\cdot]^-$ radicals appear to form a conventional degenerate system similar to a metal. This is evidenced by the relatively large electrical conductivity (the largest yet reported for an organic solid), the virtual absence of activation energy for conductivity, and the temperature-independent paramagnetism. The magnitude of the paramagnetic component of the susceptibility corresponds to a density of states at the Fermi surface of 7.5 states/ev molecule, which implies a quite narrow energy band.

In the triethylammonium salt the paramagnetic component of the magnetic susceptibility is given by

$$\chi_P = (2g^2\beta^2N/kT)[3+\exp(J/kT)]^{-1}, \qquad (1)$$

with $J = 0.041$ ev. This corresponds to an assembly of N quasi-molecules, each having a triplet state lying at an energy J above a singlet ground state. A single sharp absorption line is observed in the electron spin resonance spectrum at $g = 2.002$.[2] The temperature dependence of the intensity of this line also follows Eq. (1). The

Table I. Electronic properties of representative radical-anion salts.

Material	Electrical conductivity: Value at 300°K (ohm^{-1} cm^{-1})	Electrical conductivity: Activation energy (ev)	Magnetic susceptibility: Value at 300°K (emu-$mole^{-1}$)	Magnetic susceptibility: Temperature dependence
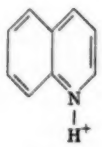 $[TCNQ\cdot]^-[TCNQ]^0$	100[a]	<0.01	$+2.2\times10^{-4}$	Decreases gradually to $+1.0\times10^{-4}$ at 77°K
$[(C_2H_5)_3NH]^+[TCNQ\cdot]^-[TCNQ]^0$	4.0[a]	0.14	$+6.4\times10^{-4}$[b]	Eq. (1) with $J=0.041$ ev
$K^+[TCNQ\cdot]^-$	1.9×10^{-4}[c]	0.36	-1.3×10^{-4}	Temperature independent from 77° to 450°K[d]

[a]In direction of highest conductivity (see text).

[b]Paramagnetic contribution.

[c]Measured on compressed powder sample.

[d]$J\sim0.15$ ev from temperature dependence of spin resonance.

electrical conductivity of this salt is highly anisotropic, having room-temperature values of 4.0, 0.05, and 0.001 $ohm^{-1}cm^{-1}$ in the three principal crystal directions and varies exponentially with temperature with an activation energy of 0.14 ev, which is isotropic within experimental error. Preliminary crystallographic results show that this salt belongs to the monoclinic $C2$ space group with four formula units per unit cell. The TCNQ units appear to be arranged in infinite face-to-face stacks with the direction of highest conductivity lying along these stacks and approximately normal to the planes of the TCNQ molecules. The thermoelectric power is -100 $\mu v/°C$ in the direction of highest conductivity, which indicates that electrons are the majority carriers in this material. We have been unable to detect a Hall voltage in this salt and estimate that such a voltage would have been observed if the electron mobility had been greater than 0.04 $cm^2/v\text{-}sec$.[3] A lower limit for the electron mobility of 0.02 $cm^2/v\text{-}sec$ can be calculated from the observed conductivity and the assumption that all of the electrons of the radical-anions participate in carrying current.

The final example in Table I, $K^+[TCNQ\cdot]^-$, provides a case in which there is a very low electrical conductivity and a relatively high activation energy for conductivity. The magnetic susceptibility is negative and temperature dependent although there are indications from spin resonance measurements of a triplet level lying ~0.15 ev above the ground state.

We are currently studying a wide range of solids containing $[TCNQ\cdot]^-$ radical-anions and will report on these in detail elsewhere.

We wish to acknowledge the assistance of Dr. Paul Arthur, Jr. in providing us with preliminary results from his crystallographic studies on some of these materials.

---

[1]D. S. Acker et al., J. Am. Chem. Soc. (to be published).

[2]D. B. Chesnut, H. Foster, and W. D. Phillips, J. Chem. Phys. (to be published).

[3]It is possible that charge carrier motion in these materials takes place by an activated hopping process, in which case it is questionable whether a Hall effect should be observed; see discussion in J. Phys. Chem. Solids 8, 50 (1959).

DIRECT OBSERVATION OF EXCITON MOTION IN CdS†

D. G. Thomas
Bell Telephone Laboratories, Murray Hill, New Jersey

and

J. J. Hopfield
Bell Telephone Laboratories, Murray Hill, New Jersey and École Normale Supérieure, Paris, France
(Received November 7, 1960)

Several authors have recently described or predicted a number of rather unusual optical effects connected with the exciton spectra of crystals. Gross and Kaplyanskii[1] have shown that the weak forbidden transition to the $n=1$ state of an exciton in cubic Cu_2O has absorption and polarization properties which depend upon the direction of the exciting light in the crystal. Pekar and Tsekvava[2] have predicted that cubic crystals can show birefringence near exciton absorption peaks if the exciton has an anisotropic mass. In CdS oriented with the hexagonal c axis perpendicular to a magnetic field H, and with the light traveling at right angles to both, Hopfield and Thomas[3] found that the exciton spectra depended markedly on the sign of H. These effects are, however, not peculiar to excitons, since quadrupole transitions of atoms in a crystal field can exhibit analogous behavior. Some effects peculiar to excitons are the result of excitons having an energy versus crystal momentum curve which is not flat. Thus Pekar[4] has shown theoretically that for wavelengths close to a suitable exciton transition, light of the same frequency and polarization can be propagated in the same direction with different refractive indices; Brodin and Pekar[5] have offered evidence of this effect in anthracene crystals at 20°K. In this Letter we report on a new experiment which gives a direct observation of the curvature of the $E(k)$ relation for excitons.

In reference 3 it was pointed out that an intrinsic direct exciton created from a photon must have the same crystal momentum vector as the photon. As a result of its momentum the exciton has a velocity $\hbar\vec{k}/M$, where $\vec{k}$ is the wave vector of the light in the medium and M is the exciton mass. In a magnetic field this velocity gives rise to an additional term in the exciton Hamiltonian equivalent to a quasi-electric field $\vec{E}_q=\hbar\vec{k}\times\vec{H}/Mc$. Stark effects on excitons are in general even functions of the electric field. This will be true for an applied electric field for $H=0$. However, in the presence of a magnetic field the effective electric field is the sum of the applied and quasi-fields. When the applied electric field, the magnetic field, and $\vec{k}$ are all mutually perpendicular the effect of the quasi-field should be to shift the plane of symmetry of the Stark effect by an amount E_q. From E_q and $\vec{k}$ the exciton mass can be directly calculated.

The Stark effect has been observed on the $n=2$ exciton states derived from the top valence band of CdS at 1.6°K in light polarized paralled to c. The Stark effect of the $n=2$ states is used since it is much larger than the effect expected for the $n=1$ states. CdS is piezoelectric and so an electric field could affect the spectra by changing the band gap; however, for all fields used no change in the positions of the $n=1$ lines could be detected, indicating that the piezoelectric effects are negligible. The crystals were 5-10 microns thick and several mm long; the electric field was applied by placing the crystals between the plates of a condenser to which a symmetrical square wave was applied, thus avoiding the necessity of making contacts. The crystals were illuminated with nearly monochromatic light from a Perkin Elmer monochromator with a mean wavelength equal to that of the exciton transition. This ensured that the crystal was exposed to the minimum light intensity so that the photoconductivity was as small as possible and the effective dielectric relaxation time as long as possible. The transmitted light was photographed with a high-dispersion Bausch and Lomb grating spectrograph; in front of the entrance slit there was a revolving sectored disk which served the dual purpose of switching the square wave by means of a separate light source and photomultiplier, and of exposing the photographic plate during only one phase of the square wave. Hence a spectrum could be observed for the electric field in either of the two possible directions.

Figure 1 shows the effect of the electric field on the separation of two pairs of lines of the Zeeman pattern of the $n=2$ exciton state in CdS with $c\perp H$ and $H=31\,000$ gauss [the symbols are identified in reference 3]. The two curves are for the two directions of H which, as explained above, give different spectra. This orientation of H with

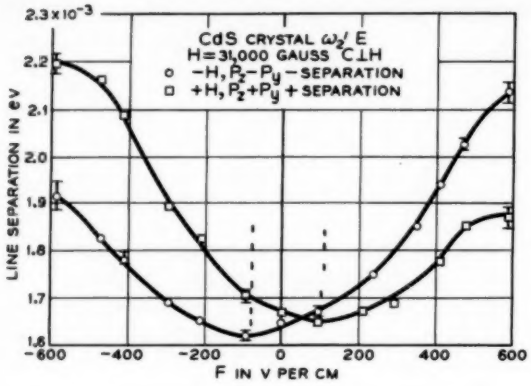

FIG. 1. The separation between two pairs of lines in the Zeeman spectra of the $n=2$ exciton state in CdS at 1.6°K, as a function of the applied electric field. The pair of lines P_z^-, P_y^- are two lines in the absorption spectrum with H in one direction, and the pair of lines P_z^+, P_y^+ are two analogous lines for H in the other direction. The light is polarized parallel to the hexagonal c axis.

respect to c was chosen as it gave the most clearly defined lines. The duration of the square-wave cycle was 400 μsec in these experiments. In order to show that the frequency is high enough to prevent appreciable screening of the electric field by polarization of the crystal, a square-wave generator was used without chopping the light. It was found that for $H=0$ there was no change in the effect as the duration was changed from 1.6 milliseconds to 20 μsec. It is seen that the two curves are approximately symmetrical with their planes of symmetry on either side of the plane of zero applied field. In the absence of a magnetic field no such asymmetry was found. The mean displacement of the planes of symmetry from the center point is about 95 ± 10 v/cm. The directions of the displacements were found to be in accord with the theory described above. At high applied electric fields the lines become broadened and there is evidence that the field in the crystal is reduced. If E_q equals 95 v/cm then M is found to be $1.1\,m_e$. (The refractive index for $E\|c$ at the frequency of the $n=2$ transition is estimated from the reflectance spectra to be 2.2; this value was used to calculate the photon momentum inside the crystal.) A recent analysis[6] of the exciton Zeeman spectra of CdS has yielded an exciton mass in a direction perpendicular to c equal to $0.9\,m_e$, where m_e is the free electron mass. The observation of the effect and its agreement in sign and approximate magnitude with the predicted values demonstrate the exciton momentum and show that this exciton "mass spectroscopy" experiment can be used to determine exciton masses.

In some crystals the Stark effect was found to be considerably larger than shown in Fig. 1 and the apparent value of E_q considerably less, in one case only 30 v/cm, although with the correct sign. These effects can be understood by supposing that at 1.6°K and 31 000 gauss in some crystals tangent (Hall angle) >1, i.e., that $\omega_c\tau>1$, where ω_c is the cyclotron resonance frequency of the highest mobility carriers (presumably electrons) and τ is the relaxation time. Under these circumstances a transverse Hall field exceeding the applied field can form across the thin dimension of the crystal in the direction of the light propagation. This field can be formed before the longitudinal field is screened out because screening of the longitudinal field by surface charge is much less efficient than that of the transverse field. Presumably at sufficiently high frequencies the Hall field would not be established, but such frequencies were not available to us. In one crystal, analysis of the results showed that $\omega_c\tau\sim1.7$. This indicates that cyclotron resonance may be observed in CdS but only in selected crystals at fields in excess of about 20 000 gauss. From the magnitude of the Stark shift shown in Fig. 1, it is estimated that $\omega_c\tau\sim0.5$ for this crystal and that the Hall field shifts the position of the symmetry planes by about 20%. The calculated exciton mass is therefore expected to be somewhat too high.

The method of determining the exciton mass described here could be of use in determining the individual masses of holes and electrons since the reduced exciton mass comes from the exciton ionization energy. Interest also derives, however, from the fact that due to polaron and other effects the exciton mass may not be simply the sum of electron and hole masses. Provided the exciton lines are sharp, which was the case for the crystal used in Fig. 1, the method is easiest to apply when $\omega_c\tau<1$. Finally, the inclusion of the $\hbar\vec{k}\times\vec{H}/Mc$ term in the Hamiltonian is of importance in analyzing the Zeeman effect of excitons, particularly for the higher quantum number exciton states.

Thanks are due to Dr. D. C. Reynolds of Wright Patterson Air Force Base for some of the crystals used in this work, and to E. A. Sadowski for

technical assistance.

†This work was supported in part by the Air Research and Development Command, U. S. Air Force.

[1]E. F. Gross and A. A. Kaplyanskii, Fiz. Tverdoga Tela U.S.S.R. 2, 379 (1960) [translation: Soviet Phys.-Solid State 2, 353 (1960)].

[2]S. I. Pekar and B. E. Tsekvava, Fiz. Tverdoga Tela U.S.S.R. 2, 261 (1960) [translation: Soviet Phys.-Solid State 2, 242 (1960)].

[3]J. J. Hopfield and D. G. Thomas, Phys. Rev. Letters 4, 357 (1960).

[4]S. I. Pekar, Zhur. Eksp. i Teoret. Fiz. 36, 451 (1959) [translation: Soviet Phys.-JETP 36(9), 314 (1959)].

[5]M. S. Brodin and S. I. Pekar, Zhur. Eksp. i Teoret. Fiz. 38, 74 (1960) [translation: Soviet Phys.-JETP, 38(11), 55 (1960)].

[6]J. J. Hopfield and D. G. Thomas (to be published).

PROTON MOTIONS IN AMMONIUM HALIDES BY SLOW NEUTRON CROSS-SECTION MEASUREMENTS*

J. J. Rush, T. I. Taylor, and W. W. Havens, Jr.
Departments of Chemistry and Physics, Columbia University, New York, New York
and Brookhaven National Laboratory, Upton, New York

(Received November 8, 1960)

The motions of ammonium ions and the order-disorder transitions in their salts have been investigated extensively by a variety of techniques. These include specific heat measurements,[1-4] crystal structure studies by neutron diffraction,[5] infrared spectroscopy,[6-8] and nuclear magnetic resonance.[9-11] The results of the investigations reported here show that cross-section measurements for neutrons of subthermal energy also provide a valuable criterion for determining the type of proton motion and the strength of chemical binding in the ammonium halides or other compounds of hydrogen.

Using a crystal spectrometer[12,13] at the Brookhaven reactor, total neutron cross-section measurements were made at room temperature for NH_3 gas at 115 psia and for the following ammonium halide salts: NH_4F, NH_4Cl, NH_4Br, and NH_4I. In Fig. 1 the cross sections per hydrogen atom, corrected for neutron absorption,[14] are plotted as a function of neutron wavelength. Since the scattering cross section for hydrogen is large and primarily incoherent, Bragg interference effects are relatively small and do not contribute significantly to the total cross section. A series of closely spaced cross-section measurements in the neighborhood of the most intense Bragg peak for NH_4Br indicated that the Bragg effects were small and could be neglected.

At short wavelengths ($\lambda_n \to 0$) the scattering cross sections approach the values for the free atoms. At long wavelengths the predominant inelastic scattering process is one in which the neutron gains energy from the crystal or molecule. The scattering cross section then becomes proportional to the wavelength, λ_n, and may be represented by $\sigma_S = a + b\lambda_n$. The slopes, b, of the cross-section curves in Fig. 1 were determined in the long-wavelength range by a least-squares fit to the data. The dashed line is the theoretical

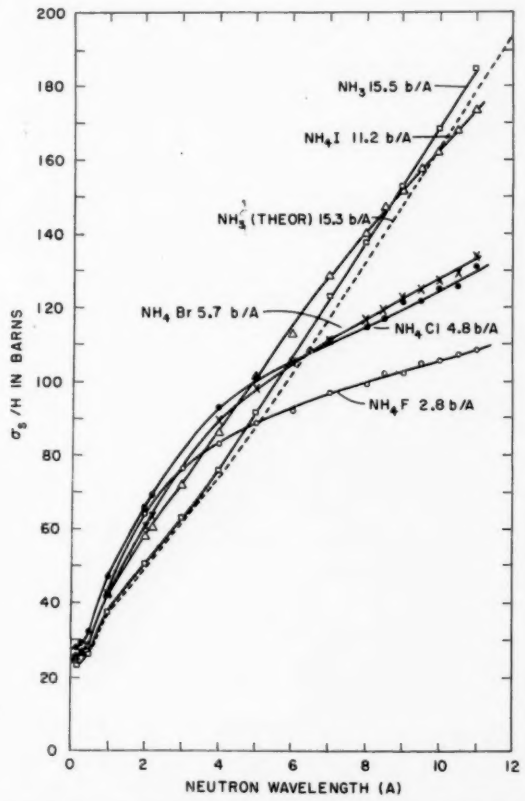

FIG. 1. Neutron scattering cross section per hydrogen atom for ammonia and the ammonium halides.

cross section per proton in NH_3 calculated using the Krieger-Nelkin method.[15]

The slopes from Fig. 1 together with other properties of the ammonium halides are summarized in Table I. Previous work referred to above has established that the ammonium ions in phases II and III may be considered torsional oscillators with the frequencies listed and with barriers to rotation[9] well above kT_λ. The transition from phase III to phase II at T_λ is a cooperative order-disorder process involving reorientation of the ammonium ions. At room temperature NH_4I is in phase I where the ammonium ions are thought to be freely rotating around the N-H--I^- axes with a potential barrier to rotation of approximately 35 cm^{-1}.[7]

The slopes and the absolute magnitudes of the scattering cross sections show a definite correlation with the proton dynamics and hydrogen bonding in the ammonium halide salts. As shown in Table I, the slopes decrease with increasing torsional frequencies, although a more detailed comparison would involve consideration of the entire fundamental and lattice vibrational spectrum. The order of the torsional frequencies and the slopes is that expected from the abilities of the halide ions to form hydrogen bonds, i.e., $F^- > Cl^- > Br^- > I^-$. Thus, the strong hydrogen bonds in ammonium fluoride result in a relatively high torsional frequency with fewer states excited and a low slope (2.85 barns/A). The weaker bonds in the other ammonium halides and a structure which allows reorientation of the ammonium ions result in higher slopes.

The slope of the scattering cross-section curve for NH_4I at room temperature approaches that for NH_3 gas. This is consistent with the model in which the ammonium ion in phase I of NH_4I is relatively free to rotate about one axis, as established from other evidence. Preliminary measurements of the slope of the cross-section curve for NH_4I at 0°C and -20°C result in values of 11 and 6 barns/A, respectively. Thus, there is a marked change in slope in passing from phase I in which the ammonium ion is freely rotating to phase II in which it is a torsional oscillator. Relatively little change was observed in passing through the order-disorder transition from phase III to phase II for NH_4Cl. It is interesting to note that the slopes for NH_4Br and NH_4Cl are measurably different even though the difference in their torsional frequencies is small. The limiting slope of the scattering cross-section curve appears to be correlated with the number of excited states and therefore the freedom of motion of the hydrogen atoms.

Table I. Limiting slopes of the scattering cross-section curves for the ammonium halides compared with other properties. The errors listed include those due to counting and to uncertainty in the absorption cross sections.[a]

	NH_4F	NH_4Cl	NH_4Br	NH_4I
Slope, barns/A, 23°C	2.85 ±0.21	4.83 ±0.18	5.71 ±0.09	11.21 ±0.18
Wavelength range, A	8–11	6–11	6–11	7–11
Cross section per proton at 10 A, barns	105	125	128	162
Motion of NH_4^+ at 23°C	osc.	osc.	osc.	rot.
Transition temperatures, °C				
Phase I (NaCl) ⟷ Phase II (CsCl)	···	184.3	137.8	-17.6
Phase II (CsCl) ⟷ Phase III[b]	···	-30.5	-38.1	-41.6
Torsional frequency, cm^{-1} [c]				
Phase III	523[b]	391	319	279
Phase II	···	359	311	···
Potential barrier to rotation[d] kcal/mole (Phase II)	···	5.3	4.2	2.9

[a] See reference 14.

[b] Phase III for NH_4Cl has the cubic CsCl structure, while that for NH_4Br and NH_4I is slightly distorted to a tetragonal structure. NH_4F has a hexagonal structure in which each NH_4^+ ion is surrounded tetrahedrally by four F^- ions. The only observed thermal transition is a small one about -30°C (references 1 and 7).

[c] See references 6 and 7.

[d] See reference 9.

The data presented here show that total cross-section measurements can give valuable evidence concerning the dynamics and chemical binding of hydrogen in molecules and crystals. Measurements are now being extended to other ammonium salts and hydrogen compounds.

*This work partially supported by the U. S. Atomic Energy Commission.

[1]F. Simon, Ann. Physik 68, 241 (1922).
[2]C. V. Simson and F. Simon, Z. physik Chem. 129, 339 (1927).
[3]L. Pauling, Phys. Rev. 36, 430 (1930).
[4]J. Fraenkel, Acta Physicochim. U.R.S.S. 3, 23 (1935).
[5]H. A. Levy and S. W. Peterson, Phys. Rev. 86, 766 (1952); J. Am. Chem. Soc. 75, 1536 (1953); J. Chem. Phys. 21, 366 (1953).
[6]E. L. Wagner and D. F. Hornig, J. Chem. Phys. 18, 296, 305 (1950).
[7]R. C. Plumb and D. F. Hornig, J. Chem. Phys. 21, 366 (1953); 23, 947 (1955).
[8]T. C. Waddington, J. Chem. Soc. 4340 (1958).
[9]H. S. Gutowsky, G. E. Pake, and R. Bersohn, J. Chem. Phys. 22, 643 (1954).
[10]L. E. Drain, Discussions Faraday Soc. 19, 200 (1955).
[11]J. A. Ibers and D. P. Stevenson, J. Chem. Phys. 28, 929 (1958).
[12]F. T. Gould, T. I. Taylor, W. W. Havens, Jr., B. M. Rustad, and E. Melkonian, Nuclear Sci. and Eng. (to be published).
[13]J. A. Moore, J. J. Rush, and B. M. Rustad, Bull. Am. Phys. Soc. 4, 245 (1959).
[14]D. J. Hughes and R. B. Schwartz, Neutron Cross Sections, Brookhaven National Laboratory Report BNL-325 (Superintendent of Documents, U. S. Government Printing Office, Washington, D. C., 1958), 2nd ed.
[15]T. J. Krieger and M. S. Nelkin, Phys. Rev. 106, 290 (1957).

ROTATING SELF-CONSISTENT FIELDS AND ROTATIONAL STATES OF NUCLEI

D. J. Thouless* and J. G. Valatin*
Institute for Theoretical Physics, University of Copenhagen, Copenhagen, Denmark
(Received October 7, 1960)

Moments of inertia of rotating nuclei have been calculated by means of the cranking model[1-3] in which the particle motion is investigated in a potential rotating with a given angular velocity. The aim of the present work is to show that the self-consistent equations of the time-dependent Hartree-Fock method have such rotating solutions. The rotating potential is produced by the particles themselves and the particles move in this potential. Similar considerations hold for the generalized Hartree-Fock equations which take into account the pairing correlations.

The time-dependent Hartree-Fock equations can be written as[4]

$$i\partial\rho/\partial t = [\nu, \rho], \tag{1a}$$

where ρ is the density matrix which satisfies the condition $\rho^2 = \rho$, and ν is the self-consistent energy. The matrix elements of ν are given by

$$\nu(x,x') = -\frac{1}{2m}\nabla^2\delta(x-x') + \int dx_1 dx_1' [(xx_1|V|x'x_1') - (xx_1|V|x_1'x')]\rho(x_1', x_1). \tag{1b}$$

For a system with translational invariance, the solutions of the time-independent equation

$$[\nu, \rho] = 0 \tag{1c}$$

are degenerate, because the center of the self-consistent potential may be moved to any position. This degeneracy permits solutions of the time-dependent equation (1a) to be constructed, which represent a translational motion of the system with constant velocity.[5] The simplest way to obtain these solutions is to transform the equations to a reference system moving with a constant velocity v. Since there are no inertial forces acting in this system, the stationary solutions in the moving system can be obtained explicitly in terms of the solutions with $v = 0$.

For a nucleus with a nonspherical equilibrium shape, the solutions of (1c) are degenerate because of an arbitrary orientation of the axes of the system. The time-dependent equation (1a) has accordingly solutions corresponding to a rotation of these axes. They can be investigated by transforming the equation to a rotating reference system. Time-independent solutions in the rotating frame represent rotating solutions in the rest system, except in the case of rotation about a symmetry axis. Transforming (1a) to a reference system rotating with uniform angular velo-

city Ω about the y axis, one obtains the equation

$$i\partial\hat{\rho}/\partial t=[\hat{\nu}+\Omega l_y,\hat{\rho}], \tag{2a}$$

where l_y is the angular momentum operator of a single particle and the notation $\hat{\rho}$, $\hat{\nu}$ indicates that these quantities are expressed in terms of variables of the rotating system. Solutions of the time-independent equation

$$[\hat{\nu}+\Omega l_y,\hat{\rho}]=0 \tag{2b}$$

will reflect the effect of the centrifugal and Coriolis forces represented by the term Ωl_y.

For small values of Ω, one can expand the solutions of (2b) in powers of Ω, by writing

$$\hat{\rho}=\hat{\rho}^{(0)}+\hat{\rho}^{(1)}+\ldots, \quad \hat{\nu}=\hat{\nu}^{(0)}+\hat{\nu}^{(1)}+\ldots \tag{3a}$$

into the equation. One has $[\hat{\nu}^{(0)},\hat{\rho}^{(0)}]=0$, and the terms linear in Ω give

$$[\hat{\nu}^{(0)},\hat{\rho}^{(1)}]+[\hat{\nu}^{(1)},\hat{\rho}^{(0)}]=-[\Omega l_y,\hat{\rho}^{(0)}]. \tag{3b}$$

The expression for $\hat{\nu}^{(1)}$ is obtained from the second term of (1b) with $\hat{\rho}$ replaced by $\hat{\rho}^{(1)}$. Assuming $\hat{\rho}^{(0)}$ and $\hat{\nu}^{(0)}$ as known, (3b) is a linear equation to determine $\hat{\rho}^{(1)}$. The moment of inertia obtained from the expression

$$\langle l_y\rangle^{(1)}=\text{trace } l_y\hat{\rho}^{(1)} \tag{3c}$$

differs from that of the cranking-model formula with independent-particle energies given by the eigenvalues of $\hat{\nu}^{(0)}$ through the correction term in $\hat{\nu}^{(1)}$. This represents the change in the rotating self-consistent potential due to the inertial forces acting on the particles.

In the representation in which $\hat{\rho}^{(0)}$, $\hat{\nu}^{(0)}$ are diagonal, (3b) is identical with equations obtained previously[6] by minimizing the ground-state energy of the Hartree-Fock method with a prescribed expectation value of a total angular momentum component. Equation (2b) would indeed result by minimizing the expectation value of the Hamiltonian in a rotating reference system, and this has the same expression as the Hamiltonian of the rest system plus a Lagrangian multiplier times an angular momentum operator. This variational problem must certainly have solutions, so steadily rotating solutions of Eq. (1a) must exist.

In the generalized Hartree-Fock method[7] the ground-state energy depends on the density matrix $\rho(x,x')$, and on the expectation value $\chi(x,x')$ of a pair of field operators. These two quantities define the components of a projection operator $\mathcal{K}$ which acts in a single-particle space of twice as many dimensions, formed by the single-particle states and their adjoints. In addition to (1b), there is a self-consistent potential determined by χ, closely related to the energy gap of the elementary excitations. The two quantities define components of a matrix $\mathfrak{M}$, and the equations of the generalized Hartree-Fock method can be written in the form[8]

$$i\partial\mathcal{K}/\partial t=[\mathfrak{M},\mathcal{K}]. \tag{4}$$

The rotating solutions of this equation result then in complete analogy to those of (1a).

---

*On leave from the Department of Mathematical Physics, University of Birmingham, Birmingham, England.

[1]D. R. Inglis, Phys. Rev. 96, 1059 (1954); 97, 701 (1955); A. Bohr and B. Mottelson, Kgl. Danske Videnskab. Selskab, Mat.fys. Medd. 30, No. 1 (1955); J. G. Valatin, Proc. Roy. Soc. (London) A238, 132 (1956).

[2]A. Bohr and B. Mottelson, Norske Videnskab. Selskab, Forhandl. 31, No. 12 (1958) (to be consulted also for further references).

[3]S. T. Belyaev, Kgl. Danske Videnskab. Selskab, Mat.fys. Medd. 31, No. 11 (1959).

[4]P. A. M. Dirac, Proc. Cambridge Phil. Soc. 26, 376 (1930).

[5]Time-dependent Slater determinant solutions of the Hartree-Fock method describing the translational motion of nuclei have been considered previously by C. van Winter (private communication).

[6]D. J. Thouless, Nuclear Phys. (to be published).

[7]J. Bardeen, L. N. Cooper, and J. R. Schrieffer, Phys. Rev. 108, 1175 (1957); J. G. Valatin, Nuovo cimento 7, 843 (1958); N. N. Bogolyubov, Nuovo cimento 7, 794 (1958); Soviet Phys.—Uspekhi 67(2), 236 (1959).

[8]J. G. Valatin (to be published).

EFFECT OF NUCLEAR ROTATION ON THE PAIRING CORRELATION

Ben R. Mottelson and J. G. Valatin*
NORDITA and The Institute for Theoretical Physics, University of Copenhagen, Copenhagen, Denmark
(Received November 8, 1960)

The empirically observed energy gap, the reduction in the effective moment of inertia below that of a rigid rotator, and the transition to spherical shape with the approach to closed shells all testify to the important role of the pairing correlation in the low excited states of deformed nuclei. The total binding energy associated with the pairing correlations is, however, quite small,[1] and thus a rather slight disturbance of the system may be sufficient to destroy the pairing and cause a transition to a less correlated particle motion.

An analogy with the correlations in superconductors has proved to be rather fruitful in interpreting the nuclear features mentioned above.[2] Pursuing this analogy, the close formal correspondence of the equations of motion in a constant magnetic field and in a rotating reference system suggests that the critical magnetic field phenomena of superconductors should also have their counterpart in the rotational spectra of nuclei. Indeed, the pairing force couples two particles in time-reversed single-particle states, and a rotation has an opposite effect on the particles forming the pair. The Coriolis forces act in opposite directions and tend to decouple the pairing correlations. This is in analogy with the effect of the magnetic forces in a metal, which act with a different sign on electrons moving in opposite directions and destroy the pairing when the field reaches a critical value. The observation or nonobservation of this effect in the rotational spectra of nuclei could serve as a test of the description of the pairing correlations in nuclei.

A suitable approximation scheme to investigate the quantum mechanics of this effect is provided by the generalized Hartree-Fock method[3] worked out in connection with the theory of superconductivity. The pairing forces are represented in this scheme by a self-consistent pairing potential, the strength of which is proportional to a gap parameter Δ. A reference system rotating with angular frequency Ω introduces a coupling term in the self-consistent energy which is Ω times the angular momentum operator l_x. The competing effect of the rotational motion and of the pairing finds its mathematical expression in the fact that Ωl_x does not commute with the pairing potential. Simple solvable models are being examined to investigate the detailed nature of the two simultaneous effects.

The main results of such a treatment can be seen from rather simple arguments. Since the Coriolis force counteracts the pairing correlations, the energy-gap parameter Δ will decrease with increasing Ω. This is reflected in an increase in the effective moment of inertia $\mathcal{I}$, and for sufficiently small Ω the effect may be described by a term in the rotational energy proportional to $I^2(I+1)^2$, where I is the rotational angular momentum. For larger values of the rotational frequency Ω, when the rotational energy is of the order of the binding energy due to the pairing correlation, the Coriolis force becomes comparable to the pairing force and gives rise to major modifications in the correlations of the particles. For Ω greater than a critical value Ω_c, the energy-gap parameter Δ vanishes and the particles perform an approximately independent motion in the average potential.

Though in the region $0<\Omega<\Omega_c$ one has a more involved intermediate coupling, the value Ω_c can independently be obtained from the simpler gap equation which results with a trial ground-state vector of the Bardeen, Cooper, Schrieffer type formed with eigenstates of the single-particle energy in the rotating system. In such a representation, the relevant matrix elements of the pairing interaction energy can be approximated by a constant which appears as an effective coupling constant so that, to second order[4] in Ω, the coupling constant G of the pairing interaction is replaced by

$$\bar{G}=G\left\{1-4\Omega^2\left\langle\sum_{k'}\left(\frac{\langle k'|l_x|k\rangle}{\epsilon_{k'}-\epsilon_k}\right)^2\right\rangle_{\mathrm{av}}\right\}. \qquad (1)$$

The energies ϵ_k and matrix elements $\langle k'|l_x|k\rangle$ refer to the one-particle states k of the nonrotating system, and the averaging is over those states k which take part in the pairing interaction. The effect of Ω is to reduce the value $\bar{G}$ of the effective coupling constant, and Ω_c is the minimum value of Ω for which the gap equation with this effective interaction leads to a vanish-

ing gap. This happens already for some finite value of $\bar{G}$. For $\Omega = 0$, the level spacing d is of the same order as the gap, and in the actual calculations carried out for the deformed nuclei[2] a reduction of G by about 30% is sufficient to cause Δ to vanish.

One can obtain an estimate of Ω_c by evaluating the averaged sum in (1), employing harmonic oscillator wave functions. For $\Delta = 0$, $\mathcal{I} = \mathcal{I}_{\text{rigid}}$, and so the critical angular momentum I_c is given by $I_c = \Omega_c \mathcal{I}_{\text{rigid}}$. One finds[5] in this way $I_c \sim 12$ for $A \sim 180$, and $I_c \sim 18$ for $A \sim 238$. These values are only slightly higher than the highest rotational states so far observed in these nuclei[6] ($I = 8$ for $A = 180$ and $I = 12$ for $A = 238$), and thus further study of high-angular-momentum states in these bands would be very interesting. One expects that in multiple Coulomb excitation studies, the rotational sequence based on the ground state will effectively terminate[7] for $I \sim I_c$. States with $I > I_c$ will have an intrinsic structure that is practically orthogonal to the ground state. One would further expect that in nuclear reaction processes populating states with $I > I_c$, the density of states as a function of I will be governed by a Boltzmann factor in which the rotational energy is given approximately by $(\hbar^2/2\mathcal{I}_{\text{rigid}})I(I+1)$ + constant, as is characteristic of a free Fermi gas.

---

*On leave from the Department of Mathematical Physics, University of Birmingham, Birmingham, England.

[1]An estimate of this energy may be obtained from the model employed in references 2 and 3. Thus, for a nucleus with an average level spacing d between the unperturbed (twofold degenerate) single-particle orbitals, one has for the total binding energy associated with the pairing correlation, including both neutrons and protons, $W = -\Delta^2/d$, where 2Δ is the magnitude of the energy gap. Inserting the empirically observed values of Δ and d gives $W \sim -1.3$ Mev for deformed nuclei, approximately independent of A.

[2]A. Bohr, B. R. Mottelson, and D. Pines, Phys. Rev. 110, 936 (1958); S. T. Belyaev, Kgl. Danske Videnskab. Selskab, Mat.-fys. Medd. 31, No. 11 (1959); A. B. Migdal, Nuclear Phys. 13, 655 (1959); Soviet Phys.—JETP 37(10), 176 (1960); J. J. Griffin and M. Rich, Phys. Rev. 118, 850 (1960); S. G. Nilsson and O. Prior, Kgl. Danske Videnskab. Selskab, Mat.-fys. Medd. (to be published); V. G. Soloviev, Doklady Akad. Nauk (U.S.S.R.) 133, 325 (1960); and J. Exptl. Theoret. Phys. (U.S.S.R.) (to be published).

[3]J. Bardeen, L. N. Cooper, and J. R. Schrieffer, Phys. Rev. 108, 1175 (1957); J. G. Valatin, Nuovo cimento 7, 843 (1958), and a paper to be published which discusses the more general equations relevant in the case of the noncommuting coupling terms which appear in the present problem. N. N. Bogolyubov, Nuovo cimento 7, 794 (1958); Soviet Phys.—Uspekhi 67(2), 236 (1959).

[4]The use of a perturbation estimate at this point is justified since $\hbar\Omega_c \ll \Delta\epsilon$, where $\Delta\epsilon$ is a typical energy denominator in (1), i.e., the rotational motion implies only a small modification in the one-particle motion although it implies a major modification in the pairing correlation. Compare also with footnote 7.

[5]One obtains essentially the same estimate for Ω_c from the condition that the difference between the rotational energies of the correlated and uncorrelated states should be equal to the energy gain $-W$ due to the correlation.

[6]For the rotational band of Hf^{178} and Hf^{180}, see, e.g., D. Strominger, J. M. Hollander, and G. T. Seaborg, Revs. Modern Phys. 30, 585 (1958); for U^{238} see F. Stephens, R. Diamond, and I. Perlman, Phys. Rev. Letters 3, 435 (1959).

[7]It should be emphasized that the effect considered here is quite distinct from the modifications in the rotational motion that occur when the rotational frequency becomes of the order of the intrinsic particle frequencies. These latter modifications effectively terminate the rotational bands when $I \sim I_m$, where I_m is the maximum angular momentum that can be constructed out of the available single-particle configurations [see J. P. Elliott, Proc. Roy. Soc. (London) A245, 128 (1958)]. For the heavy nuclei which exhibit well-defined rotational band structure, $I_m \sim 40$.

INTERPRETATION OF THE BERKELEY ANOMALY IN HIGH-ENERGY p - d COLLISIONS*

Arnold Tubis and Jack L. Uretsky
Physics Department, Purdue University, Lafayette, Indiana
(Received October 31, 1960)

We should like to offer an alternate explanation of the "bump" observed in the recent Berkeley experiments[1] on double-pion production in proton-deuteron collisions. It will be recalled that these experiments consisted of an examination of the momentum spectrum of the final He^3 or H^3 nucleus at a fixed laboratory angle and in a momentum range corresponding to double-pion production. Evidence was found for a strong peaking in the momentum spectrum of the final nucleus at a momentum corresponding to a total energy of about 310 Mev of the two pions in their own center-of-momentum system. Abashian et al. found that they could fit this peaking to a p-wave resonance in the $T=1$ state of the outgoing meson pair.

We shall proceed according to the rules set up in reference 1; that is to say, we shall consider a generalization of the statistical model to allow for p-wave scattering between the final-state mesons. We do this by writing the production matrix element,[2] in the system where the center-of-momentum of the two pions is at rest, in the form

$$\mathfrak{M}'(\vec{q}) = M\vec{q}\cdot\vec{\lambda}_3, \tag{1}$$

where M is a constant, $\vec{q}$ the momentum of one of the pions, and $\vec{\lambda}_3$ the momentum of the final nucleus. Final-state scattering is accounted for by writing the total matrix element as

$$\mathfrak{M}(\vec{q}) = \int d^3q'\ \psi^*(\vec{q},\vec{q}')\mathfrak{M}'(\vec{q}'). \tag{2}$$

The wave function $\psi^*(\vec{q},\vec{q}')$ describes the elastic π - π scattering from a state of relative momentum $\vec{q}'$ to one of momentum $\vec{q}$. We use the asymptotic form of the wave function (in configuration space) and invoke a minimum "radius of interaction," R. The transition probability is then found to be

$$d^2W/dp_3d\Omega_3 \propto p_3^{\,2}\lambda_3^{\,2}E_3^{\,-1}t[(t-4)/t]^{3/2}$$

$$\times(q^3\cot\delta_1 - R^{-3})^2\,(q^6\cot^2\delta_1 + q^6)^{-1}. \tag{3}$$

The last equation introduces p_3 and E_3, the laboratory momentum and energy, respectively, of the outgoing nucleon, t is the square of the energy of the two outgoing pions in their own rest system in units of the pion mass, and δ_1 is the π - π p-wave scattering phase shift for a c.m. energy of $\sqrt{t}$. Let us now make the simplest possible assumption concerning $\cot\delta_1$, namely that the scattering length approximation is valid over most of the energy range in question. We write, then, that

$$q^3\cot\delta_1 = a^{-3}, \tag{4}$$

and choose the scattering length, a, to give the production cross section a maximum at about 300-Mev total energy in the two-pion rest system. The scattering length turns out to be about 2.5 meson Compton wavelengths. The corresponding momentum dependence of the outgoing nucleus ($T_{\text{proton}} = 743$ Mev) is shown in the solid curve of Fig. 1. The dashed curve, shown for

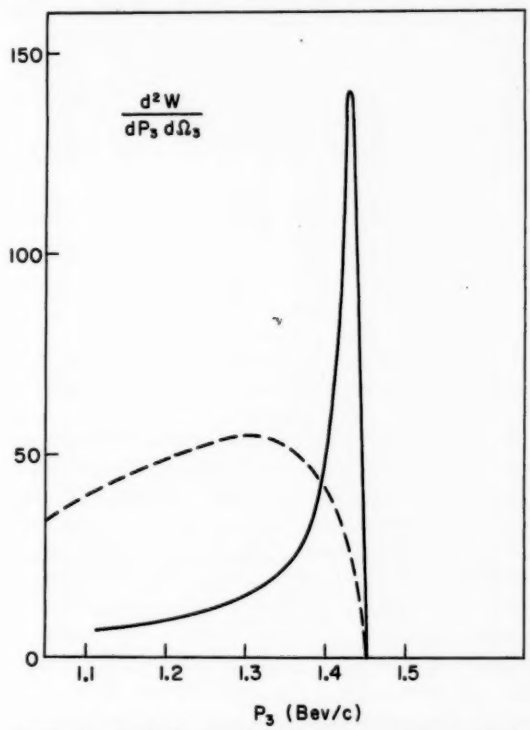

FIG. 1. Contribution of the $T=1$ two-pion production mode to the He^3 or H^3 momentum distribution function as given by Eqs. (3) and (4). The solid curve corresponds to a scattering length a of 2.5 pion Compton wavelengths while the dashed curve corresponds to a zero scattering length. The distribution functions are evaluated for an incident proton energy of 743 Mev in the laboratory and are to be compared with Figs. 3 and 4 of Abashian et al.[1] We have used arbitrary units for the ordinate scale.

purpose of comparison, corresponds to the "p-wave statistical model" obtained by allowing the scattering length to vanish.

It is our feeling that the present Berkeley data are consistent with the scattering-length model we have presented and that there is no necessity for invoking the existence of a resonance to explain the Berkeley "bumps." The validity of our approximation rests upon the assumption that the effective range and higher terms in the expansion implied by Eq. (4) are sufficiently small to warrant their neglect in the energy range under consideration. We note that if this is the case, and if the appropriate choice of signs is made for the effective-range term, it is possible, within the framework of our model, to have a high-energy resonance such as the one required by Frazer and Fulco[3] although its shape will not satisfy their requirements.

If the explanation we propose is found to be consistent with future experiments, it raises the possibility of an interesting speculation. We recall that[4] if there is a bound p state of binding energy E_B, and if the terms involving higher powers of q^2 in the expression for $\cot\delta_1$ are sufficiently small, then the binding energy is related to the scattering length by the relation ($\hbar = \mu = c = 1$)

$$E_B \approx 1/a.$$

Thus, if the scattering length in our model can be shown to be positive, we are led to consideration of a particle that is a two-meson bound state of spin and isotopic spin 1 and of a mass about equal to 450 electron masses.[5]

*This work was supported in part by the Air Force Office of Scientific Research and the U. S. Atomic Energy Commission.

[1]A. Abashian, N. E. Booth, and K. M. Crowe, Phys. Rev. Letters 5, 258 (1960).

[2]Julius S. Kovacs, Phys. Rev. 101, 397 (1956).

[3]W. R. Frazer and J. R. Fulco, Phys. Rev. Letters 2, 365 (1959).

[4]L. D. Landau and E. M. Lifshitz, Quantum Mechanics (Pergamon Press, New York, 1958), pp. 401-2.

[5]J. L. Uretsky and T. R. Palfrey (to be published) have considered the possibility of finding a two-meson bound s-state in photoproduction. In that paper the conclusion is reached that there is at present no persuasive evidence contradicting the existence of a two-meson bound state.

RESONANT SCATTERING OF ANTINEUTRINOS

J. C. Barton
Department of Physics, Northern Polytechnic, London, England
(Received October 27, 1960)

It has recently been suggested by Glashow[1] that there might be a resonance in the scattering of antineutrinos by electrons which would lead to an appreciable production of μ mesons. It was estimated that (under the hypothesis of an intermediate charged boson of mass m_Z) the antineutrinos in the cosmic radiation would produce a meson flux of from 0.1 m^{-2} day^{-1} (for m_Z = nucleon mass) to 2 m^{-2} day^{-1} (for m_Z = K-meson mass); this rate should be independent of the depth below ground and should thus be distinguishable from mesons produced in the atmosphere.

While studying the intensity of cosmic radiation at various depths underground, a recorder of geometric area 0.08 m^2 has been operated for 21 days at a depth of 5050 m.w.e. No cosmic-ray events were observed. The effective area of the recorder for high-energy mesons, which would be accompanied by knockon and pair-produced electrons, is at least 25% greater than the geometric area so that the meson flux is probably less than 0.5 m^{-2} day^{-1}. According to Glashow's theory this result makes it unlikely that there is a resonance involving a virtual charged boson with mass equal to that of a K meson.

[1]S. L. Glashow, Phys. Rev. 118, 316 (1960).

MUONIUM FORMATION IN SEMICONDUCTORS*

G. Feher†
Bell Telephone Laboratories, Murray Hill, New Jersey and Columbia University, New York, New York

and

R. Prepost and A. M. Sachs
Columbia University, New York, New York
(Received November 4, 1960)

A well-known consequence of parity nonconservation in π - μ decay[1] is the longitudinal spin polarization of muons in meson beams emerging from synchrocyclotrons.[2] The residual polarization of positive muons before decaying in various solids in which they have been stopped has been measured by several groups.[3-5] In some substances (e.g., graphite, metals) no depolarization occurs; in others (e.g., nuclear emulsions, polyethylene) a partial depolarization has been observed; while in a few (e.g., SiO_2) there is complete depolarization. The details of the processes involved are at present not understood. However, measurements including the quenching of depolarization in external longitudinal fields[6-11] are consistent with a mechanism in which the muon undergoes short-lived attachments to electrons; i.e., μ^+e^- systems called muonium are formed. In order to gain a better understanding of these processes we have studied the depolarization in semiconductors, the electronic structure of which is well understood, and the electronic concentration of which can be easily varied. In this Letter we report on the depolarization of muons in silicon and germanium, and in particular show that by varying the concentration of impurities, the entire range between maximum and essentially zero polarization can be covered.

The polarization of the muons is detected by measuring the asymmetry in the angular distribution of positrons from the muon decay. This is accomplished by a standard precession-type experiment, as illustrated in Fig. 1. Five scintillation counters were placed in the "85-Mev" external positive-meson beam of the Nevis synchrocyclotron. Sufficient absorber was placed between counters 1 and 2 to absorb the pions and allow the muons in the beam to stop in the target material placed between counters 3 and 4. Forward decay positrons in counter pair 23 and backward positrons in 45 were counted during a gate 1.2 μsec long, which was started 0.6 μsec after each stopped muon. Alternate measurements were taken in one case with no applied external field and in another where the muon spins were precessed through an average angle of 180 deg in a 40-gauss vertical field provided by a set of Helmholtz coils.

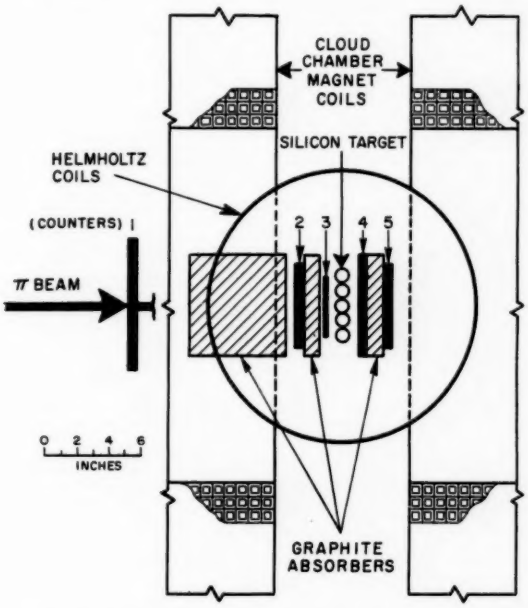

FIG. 1. Experimental arrangement for measuring the depolarization of muons. Cloud-chamber magnet coils are used in experiments to measure the quenching of muon depolarization in large longitudinal fields. Helmholtz coils provide the transverse field in which the muons precess through 180 deg.

Each target was assembled from cylindrical samples with the desired impurity concentration. The effective target sizes ranged from $2\frac{1}{2}$in. $\times 2\frac{1}{2}$in. $\times\frac{1}{2}$in. to 5in. $\times$ 5in. $\times$ 1in. The targets were imbedded in Styrofoam holders which positioned the samples in addition to serving as Dewars for cooling to liquid nitrogen temperatures.

The experimental results are shown in Fig. 2, where the usual positron asymmetry parameter, a, is plotted against the concentration of free electrons and holes in silicon. The results on a single sample of n-type germanium and of graph-

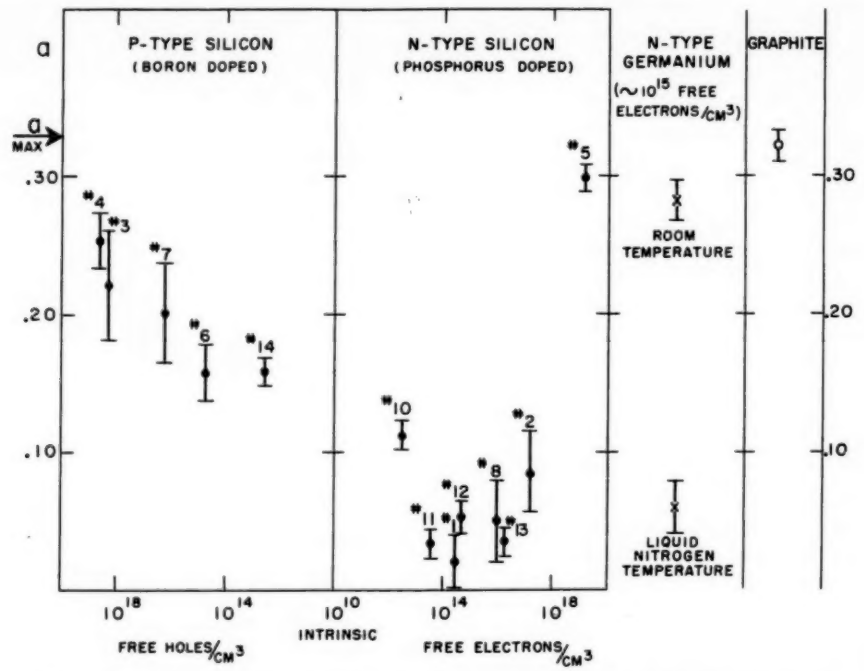

FIG. 2. Experimental values of the asymmetry parameter, a, for decay positrons from stopped muons (a) versus free electron concentration in n-type silicon and free hole concentration in p-type silicon; (b) in one sample of n-type germanium (phosphorus-doped) at room temperature and liquid nitrogen temperature; and (c) in a graphite sample for which the maximum value of $a = 0.33$ is assumed to correspond to full muon polarization. The abscissas for n-type and p-type silicon have been joined at the value of the intrinsic concentration for room temperature ($\sim 10^{10}$ cm^{-3}). Since the product of the numbers of free holes and electrons in thermal equilibrium with the lattice is constant at a given temperature (i.e., $\sim 10^{20}$ for silicon at room temperature), the entire abscissa represents an increasing free electron concentration to the right (or an increasing hole concentration to the left).

ite are shown on the same graph. The angular distribution of decay positrons is of the form $1 - a\cos\theta$, where θ is the angle between the directions of the incident muons and the emitted positrons. In order to obtain a from the measured peak-to-valley ratios for forward and backward positrons, corrections have been made for accidental counts, for positrons not originating in the target, and for smearing caused by the finite gate width used and acceptance angle subtended by the detectors.

Before discussing the results, it may be recalled that embedding impurity atoms such as phosphorus in a material with a large dielectric constant ϵ, such as silicon, creates what are called "shallow donors."[12] The donor impurities have hydrogen-like orbits of greatly expanded radius, an ionization energy reduced by $\sim\epsilon^2$, and markedly reduced hyperfine interactions. For example, phosphorus in silicon has an ionization energy $E_i = 0.045$ ev, and the hyperfine interaction of its electron is approximately 30 times smaller than it would be if ϵ were unity.[13] Therefore, if muonium is formed in silicon or germanium, one might expect it to behave like a shallow donor, with reduced ionization energy and hyperfine interaction. The experimental results will be discussed with this point of view in mind.

The free electrons and holes are supplied by the added impurities which are almost all ionized at room temperature.[14] The time τ_B that the electron is bound to a donor (i.e., the lifetime of the muonium state) can be shown to be

$$\tau_B = (\sigma v N_C)^{-1} \exp(E_i/kT), \qquad (1)$$

where σ is the capture cross section of an ionized donor, v is the velocity of an electron, N_C is the density of states in the conduction band, E_i is the ionization energy of the impurity, and kT is the thermal energy of the carriers.[15] For donor concentrations exceeding 10^{18} per cm^3, the donor wave functions overlap, the electrons are no longer localized, the effective τ_B becomes much shorter than given by Eq. (1), and one approaches a state similar to a metal (see Fig. 16 of reference 8). This situation is exemplified by sample No. 5 which like graphite shows no depolarization, corresponding to the lack of muonium formation. As the donor concentration is reduced, the electrons are able to attach themselves for a time τ_B to the muon. This results in the depolarization exhibited by samples 2, 13, 8, 12, 1, and 11. As the donor concentration is further decreased and acceptors are added, the equilibrium number of electrons becomes too small to have a significant probability to form muonium.[16] The partial depolarization observed (see samples 10, 14, and 6) must therefore be due to the capture of electrons that are not in equilibrium with the lattice but may be created, for example, by the muon passing through the sample. The weak dependence of a on the hole concentration is at present not understood.

A germanium sample with $\sim 10^{15}$ elec/cm^3 showed only a very small degree of depolarization (see Fig. 2). This presumably results from the fact that the ionization energy of donors in germanium is four times smaller than in silicon, resulting in a decrease in τ_B [see Eq. (1)]. By going to 77°K, the relevant ratio of E_i/kT equals that of silicon at room temperature and indeed an almost complete depolarization (similar to that for silicon) is observed (see Fig. 2).

The polarization may be re-established by applying a longitudinal magnetic field to the sample.[6-11] We have performed a preliminary experiment on sample 11 and found that a field of approximately 1000 gauss quenched half of the muon depolarization. This is consistent with the idea of shallow donor formations if the number of (μ^+e^-) attachments with the reduced hyperfine interaction formed in a muon lifetime is of the order of a hundred.[17] Further depolarization experiments at low temperatures are in progress.

We would like to thank T. Benedict of Merck & Company, Inc. and several members of the Bell Telephone Laboratories for supplying the samples used in these experiments, and would also like to thank P. W. Anderson for stimulating discussions. We are indebted to L. Levine, P. Nemethy, and J. Sunderland for aid in the measurements.

---

*This research is supported by the Office of Naval Research and the U. S. Atomic Energy Commission.

†Present address: University of California, La Jolla, California.

[1]T. D. Lee and C. N. Yang, Phys. Rev. 104, 254 (1956).

[2]R. L. Garwin, L. M. Lederman, and M. Weinrich, Phys. Rev. 105, 1415 (1957).

[3]D. Berley, T. Coffin, R. L. Garwin, L. M. Lederman, and M. Weinrich, Bull. Am. Phys. Soc. 2, 204 (1957).

[4]R. A. Swanson, N. P. Campbell, E. L. Garwin, J. C. Sens, V. L. Telegdi, S. C. Wright, and D. D. Yovanovitch, Bull. Am. Phys. Soc. 2, 205 (1957).

[5]R. A. Swanson, Phys. Rev. 112, 580 (1958).

[6]J. Orear, G. Harris, and E. Bierman, Phys. Rev. 107, 322 (1957).

[7]W. H. Barkas, P. C. Giles, H. H. Heckman, F. W. Inman, and F. M. Smith, Phys. Rev. 107, 911 (1957).

[8]J. Sens, R. A. Swanson, V. L. Telegdi, and D. D. Yovanovitch, Phys. Rev. 107, 1465 (1957).

[9]S. A. Ali-Zade, I. I. Gurevich, U. P. Dobretzov, B. A. Nikol'skii, and L. V. Surkova, J. Exptl. Theoret. Phys. U.S.S.R. 36, 1327 (1959)[translation: Soviet Phys.-JETP 9, 940 (1959)].

[10]G. R. Lynch, J. Orear, and S. Rosendorff, Phys. Rev. 118, 284 (1960).

[11]A. O. Vaisenberg, N. V. Rabin, and V. A. Smirnitskii, J. Exptl. Theoret. Phys. U.S.S.R. 36, 1680 (1959)[translation: Soviet Phys.-JETP 9, 1197 (1959)].

[12]For a review on this subject, see W. Kohn, in Solid-State Physics, edited by F. Seitz and D. Turnbull (Academic Press, Inc., New York, 1957), Vol. 5.

[13]G. Feher, Phys. Rev. 114, 1219 (1959).

[14]The fraction of un-ionized impurities is given by $(N_D^+/N_C)\exp(E_i/kT)$, where N_D^+ is the number of ionized donors (or acceptors), the rest of the symbols being defined in the text.

[15]Taking $\sigma = 10^{-15}$ cm^2 [see M. Lax, Phys. Rev. 119, 1502 (1960)] one obtains for silicon at room temperature $\tau_B \simeq 4 \times 10^{-11}$ sec.

[16]The trapping time τ_t for an electron is given by $\tau_t = (\sigma v n)^{-1}$, where n is the number of available electrons. For an intrinsic silicon sample with $\sim 10^{10}$ elec/cm^3, τ_t becomes $\sim 10^{-2}$ sec too long to account for the observed depolarization.

[17]R. A. Ferrell, Y. C. Lee, and M. K. Pal, Phys. Rev. 118, 317 (1960).

PHOTOPRODUCTION OF NEGATIVE PIONS FROM HYDROGEN AT FORWARD ANGLES*

J. R. Kilner, R. E. Diebold, and R. L. Walker
California Institute of Technology, Pasadena, California
(Received November 3, 1960)

The recent theoretical investigation by Drell[1] of the photoproduction of very high energy particles at small angles predicts a large peak in the differential cross section in this region. In particular, if one applies his results to the photoproduction of negative pions from hydrogen one obtains a value for the differential cross section that is several times larger than the value measured in pair production experiments at larger angles and lower energies. This interesting result has prompted the experimental investigation reported here.

The bremsstrahlung beam from the CalTech synchrotron was used to produce negative pions in a liquid hydrogen target predominantly through the process

$$\gamma + p \rightarrow \pi^- + \pi^+ + p. \qquad (1)$$

This is the only process kinematically possible for Q less than 140 Mev, where Q is the total kinetic energy in the p - π^+ center-of-momentum system. Above $Q = 140$ Mev, the π^- may be produced by

$$\gamma + p \rightarrow \pi^- + \begin{cases} \pi^+ + p + \pi^0 \\ \pi^+ + n + \pi^+; \end{cases} \qquad (2)$$

however, Chasan et al.[2] indicate that the cross section for this process is small, especially near the threshold.

Since there are three or more particles in the final state it was necessary to perform a "synchrotron subtraction" to determine the energy, k, of the photon initiating the reaction. An interval of approximately 100 Mev centered at 1230 Mev was obtained by taking the difference in normalized counting rates at peak bremsstrahlung energies of 1300 and 1200 Mev.

The negative pions were analyzed with a wedge-type magnetic spectrometer and detected with a counter telescope system consisting of one Čerenkov and three scintillation counters with a fifth "aperture-defining" counter located at the magnet exit. Pole-face veto counters were used to eliminate particles scattering from the magnet. Accidental and cosmic-ray counting rates were negligible. Brody et al.[3] give a more complete description of the apparatus except that we used the same magnet in the "high-energy" position as described by Vette.[4]

Data were taken at laboratory angles ranging from five to thirty degrees and π^- laboratory momenta ranging from approximately 600 to 1000 Mev/c. At laboratory angles less than about ten degrees appreciable numbers of electrons traversed the system and were rejected using the fact that they produce showers in matter. A one-half inch lead converter was placed in front of each of the last two counters, and the "electron biases" on the pulses from these counters were adjusted so that about 95% of the electrons and only 8% of the pions would give a pulse above this bias. Although there were approximately three times as many electrons as pions at the most forward points measured, the largest resulting electron contaminations were only on the order of 20% because of the high electron detection efficiency.

The data were further corrected for empty target backgrounds, pion decay in flight,[5] μ contamination from the π - μ decay,[5] and absorption in the system.[5] The photon beam was monitored by ionization chambers calibrated with an energy-independent Quantameter.[6] The error in this calibration and all other systematic errors (amounting to perhaps 5%) are not included in the graphs where only the statistical counting errors are shown.

The experimental differential cross sections, $\sigma(\theta, \omega)$, for $k = 1230$ Mev, are shown in Fig. 1 as a function of π^- center-of-momentum total energy (and also of Q) for several angles.[7] Not shown are four points for $\omega = 370$ Mev ($Q = 293$ Mev) with very large statistical errors, which gave values of $\sigma(\theta, \omega)$ consistent with other values near the lower energy end. Figure 2 gives the angular distribution for the average value of the data points at $\omega = 464$, $\omega = 505$, and $\omega = 519$ Mev. The peak value of the cross section is approximately five times larger than the pair production cross sections at lower energies and backward angles.[8] However, the peak is rather narrow in both energy and angle so that it contributes only about 25% of the total cross section. Specifically, the region of the peak, $10° \leq \theta \leq 55°$ and $420 \leq \omega \leq 573$ Mev in the center-of-momentum system, contributes 13 μb to the total cross section of about 50 μb.[2,8]

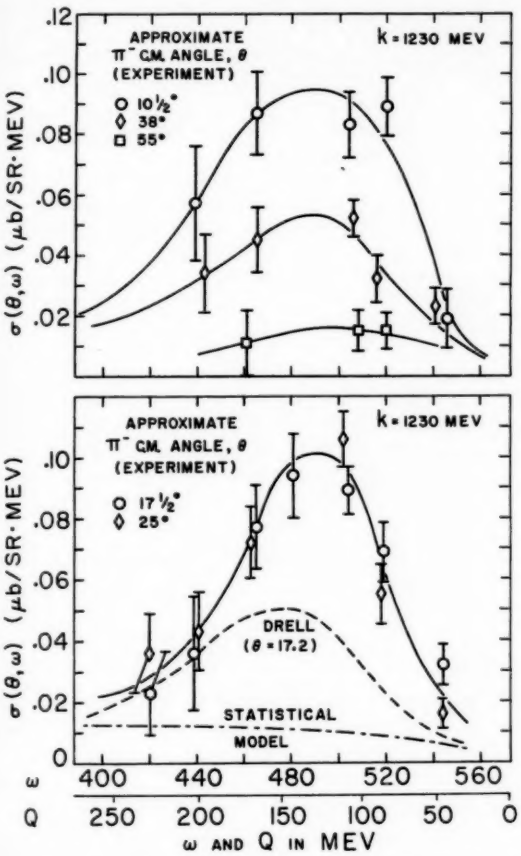

FIG. 1. The differential cross section as a function of ω (or Q) for several fixed angles. $\sigma(\theta,\omega)d\Omega\,d\omega$ is the cross section for producing a π^- at angle θ within $d\Omega$ and total energy ω within $d\omega$, all in the center-of-momentum system. The solid curves are drawn to fit the experimental points. The dashed curves are calculated from Drell's model (for $\theta = 17.2$ degrees) and for an isotropic statistical model, which are described in the text. Experimental resolutions have been folded in.

Drell[1] gives the diagram shown in Fig. 3 as the main contributor at forward angles for high-energy π^- photoproduction. The differential cross section is given by[9]

$$\sigma(\theta,\omega)d\Omega\,d\omega = \frac{\alpha}{2\pi}\frac{\sin^2\theta}{(1-\beta\cos\theta)^2}\frac{d\Omega}{4\pi}\frac{\omega(k-\omega)d\omega}{k^3}\sigma_{\pi^+ + p}(Q). \quad (3)$$

The case when more than one pion emerges from vertex (b) of Fig. 3 is included since this is contained in the total cross section,[10] $\sigma_{\pi^+ + p}(Q)$. Drell's process may be particularly easy to recognize in hydrogen where it should show not only the characteristic forward angle peak, but also a strongly peaked energy dependence arising from the 3-3 resonance in $\sigma_{\pi^+ + p}(Q)$.

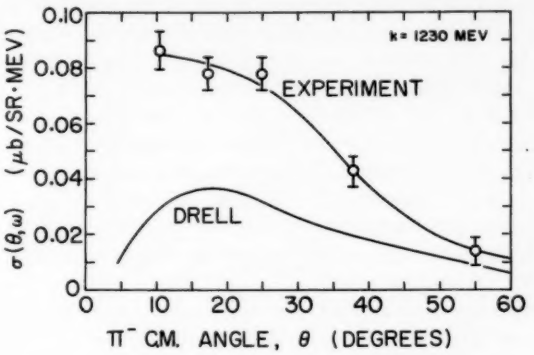

FIG. 2. The angular distribution for the average value of points at $\omega = 464$, $\omega = 505$, and $\omega = 519$ Mev. The prediction of the Drell model averaged in the same manner is also shown with the experimental resolutions folded in.

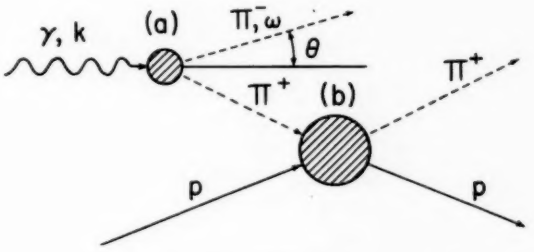

FIG. 3. The diagram for the photoproduction of negative pions which gives a large contribution at high energy and forward angles. Equation (3) gives the cross section from this diagram.

The cross section calculated from Eq. (3) is shown in Fig. 1 for $\theta = 17.2$ degrees and in Fig. 2 where the same average used for the data points is plotted. Both of these curves have the photon distribution and magnet resolutions folded in. The data show the expected effect of the pion-nucleon scattering resonance which has a peak at $Q \approx 145$ Mev. Of course, any "isobar model" would give a similar dependence of $\sigma(\theta,\omega)$ on ω, but the fact that the angular distribution decreases so rapidly with angle is probably more specific to Drell's process. The distribution predicted

by an isotropic statistical model[11] normalized to a total cross section[2,8] of 50 μb is also shown in Fig. 1.

Qualitatively, our results agree rather well with Drell's model, although the experimental cross sections are in general considerably larger than those calculated from Eq. (3), and do not show any decrease at the smallest angle measured. One should perhaps not expect a better quantitative agreement since Drell's diagram of Fig. 3 is not the only one leading to pion pair production, and other relatively small amplitudes may produce appreciable effects by interference with the Drell term.

*This work was supported in part by the U. S. Atomic Energy Commission.

[1]S. D. Drell, Phys. Rev. Letters 5, 278 (1960).

[2]B. M. Chasan, G. Cocconi, V. T. Cocconi, R. M. Schectman, and D. H. White, Phys. Rev. 119, 811 (1960).

[3]H. M. Brody, A. M. Wetherell, and R. L. Walker, Phys. Rev. 119, 1710 (1960).

[4]J. I. Vette, Phys. Rev. 111, 622 (1958).

[5]J. H. Boyden, Ph.D. thesis, California Institute of Technology, 1961 (unpublished).

[6]R. R. Wilson, Nuclear Instr. 1, 101 (1957).

[7]$\sigma(\theta,\omega)d\Omega\,d\omega$ is the cross section for producting a π^- at an angle θ and an energy ω within the intervals $d\Omega$ and $d\omega$.

[8]M. Bloch and M. Sands, Phys. Rev. 113, 305 (1959).

[9]This is Eq. (2) of reference 1 with $\sigma_{\pi^+ + p}(k-\omega)$ replaced by $\sigma_{\pi^+ + p}(Q)$.

[10]$\sigma_{\pi^+ + p}(Q)$ is from S. J. Lindenbaum and L. C. L. Yuan, Phys. Rev. 100, 306 (1955), and Phys. Rev. 111, 1380 (1958); R. Cool, O. Piccioni, and D. Clark, Phys. Rev. 103, 1082 (1956); S. W. Barnes, B. Rose, G. Giacomelli, J. Ring, K. Miyake, and K. Kinsey, Phys. Rev. 117, 226 (1960).

[11]Extrapolated from curves given in reference 8.

RESONANCE IN THE $\Lambda\pi$ SYSTEM*

Margaret Alston, Luis W. Alvarez, Philippe Eberhard,† Myron L. Good,‡
William Graziano, Harold K. Ticho,‖ and Stanley G. Wojcicki
Lawrence Radiation Laboratory and Department of Physics, University of California, Berkeley, California
(Received October 31, 1960)

We report a study of the reaction

$$K^- + p \rightarrow \Lambda^0 + \pi^+ + \pi^- \qquad (1)$$

produced by 1.15-Bev/c K^- mesons and observed in the Lawrence Radiation Laboratory's 15-in. hydrogen bubble chamber. A preliminary report of these results was presented at the 1960 Rochester Conference.[1] The beam was purified by two velocity spectrometers.[2] A Ξ^0 hyperon observed during the run[3] and the preliminary cross sections[4] for various K^- reactions at 1.15 Bev/c have been reported previously. Reaction (1) was the first one selected for detailed study, because it appeared to take place with relatively large probability and because the event, a 2-prong interaction accompanied by a V, was easily identified. In a volume of the chamber sufficiently restricted so that the scanning efficiency was near 100%, 255 such events were found. These events were measured, and the track data supplied to a computer which tested each event for goodness of fit to various kinematic hypotheses. The possible reactions, the distribution of events, and the corresponding cross sections are given in Table I. An event was placed in a given category of Table I if the χ^2 probability for the other hypotheses was $<1\%$. It appears likely that the majority of the events in group (e) are also reactions of type (1). This belief is based on the following arguments:

1. Since the kinematics of a $\Lambda\pi\pi$ fit (four constraints) are more overdetermined than those of a $\Sigma^0\pi\pi$ fit (two constraints), it is relatively easy for a $\Lambda\pi\pi$ reaction to fit a $\Sigma^0\pi\pi$ reaction, but only

Table I. Distribution of events among different reactions.

Reaction	No. of events	Cross section (mb)
(a) $K^- + p \rightarrow \bar{K}^0 + p + \pi^-$	48	2.0 ± 0.3
(b) $K^- + p \rightarrow (\Lambda \text{ or } \Sigma^0) + \pi^+ + \pi^- + \pi^0$	39	1.1 ± 0.2
(c) $K^- + p \rightarrow \Sigma^0 + \pi^+ + \pi^-$	27	
(d) $K^- + p \rightarrow \Lambda + \pi^+ + \pi^-$	49	4.1 ± 0.4
(e) $K^- + p \rightarrow (\Lambda \text{ or } \Sigma^0) + \pi^+ + \pi^-$	92	
Total	255	7.2 ± 0.5

very few Σ^0 configurations can fit the $\Lambda\pi\pi$ reactions.

2. The events of group (e) when treated as $\Sigma^0\pi\pi$ reactions give a χ^2 distribution which is much worse than that obtained when they are treated as $\Lambda\pi\pi$ reactions.

In what follows, the 141 events of groups (d) and (e) are treated as examples of reaction (1). We estimate that 10 to 15% are actually Σ^0 events.

The energy distribution of the two pions in the K^--p barycentric system is shown in Fig. 1. If the cross section were dominated by phase space alone, the distribution of the points on the two-dimensional plot of Fig. 1 should be uniform. This is clearly not the case. On the contrary, both the π^+ and the π^- distributions have peaks near 285 Mev, such as would be expected from a quasi-two-body reaction of the type

$$K^- + p \rightarrow Y^{*\pm} + \pi^{\mp}, \qquad (2)$$

the Y^* having a mass spectrum peaking at ~1380 Mev. If the Y^* of mass 1380 Mev breaks up according to

$$Y^{*\pm} \rightarrow \Lambda^0 + \pi^{\pm}, \qquad (3)$$

the pions from this breakup are expected to have energies ranging from 58 to 175 Mev in the K^-p rest system. Those pions from (3) are well separated from the pions arising from reaction (2) in the energy histograms.

The isotopic spin of this excited hyperon must be one, since it breaks up into a Λ and a π. Since the Y^* is produced with a pion, also of isotopic spin one, the reaction could proceed either in the $I=0$ or the $I=1$ state. Therefore the ratio of Y^{*+} to Y^{*-} will depend on the relative magnitude and phase of the two isotopic-spin amplitudes and thus could differ from unity. We observed 59 Y^{*+} events and 82 Y^{*-} events, using the criterion for separation that the high-momentum π meson is the pion from reaction (2).

Figure 2 shows the distribution in mass of the Y^* state (both Y^{*+} and Y^{*-}) including all 141 events, again using the higher energy pion in each event to calculate the Y^* mass. The experimental uncertainty in the mass for each event is small compared to the observed width of the curve. The curves of Fig. 2 are discussed later.

Figure 3 shows production angular distributions for Y^{*+} and Y^{*-} in the K^-p rest system. Partial waves with $l>0$ appear to be present, as would be expected since $\hbar k/m_\pi c$ approximately equals 3. The difference between the Y^{*+} and Y^{*-} angular distributions may reflect the different superposi-

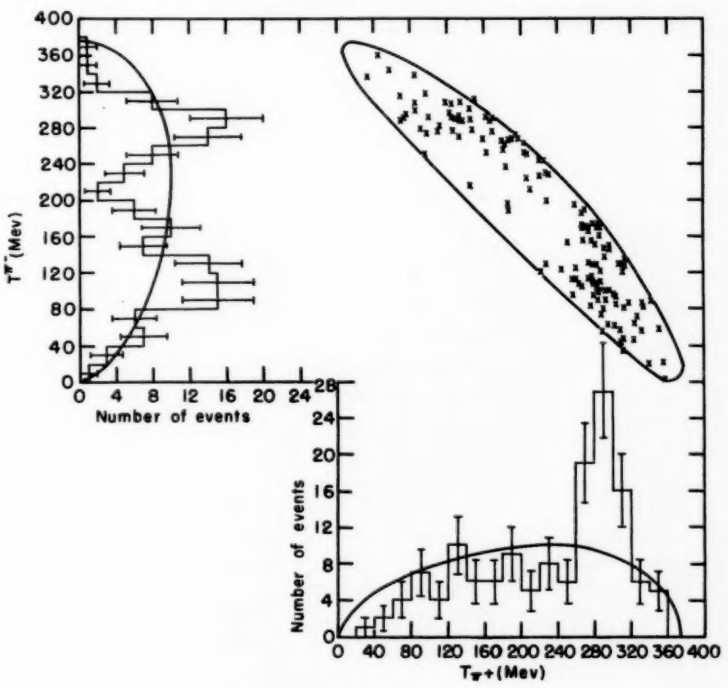

FIG. 1. Energy distribution of the two pions from the reaction $K^-+p \rightarrow \Lambda+\pi^++\pi^-$. Each event is plotted only once on the Dalitz plot, which should be uniformly populated if phase space dominated the reaction. The two energy histograms are merely one-dimensional projections of the two-dimensional plot, and each event is represented once on each histogram. The solid lines superimposed over the histograms are the phase-space curves.

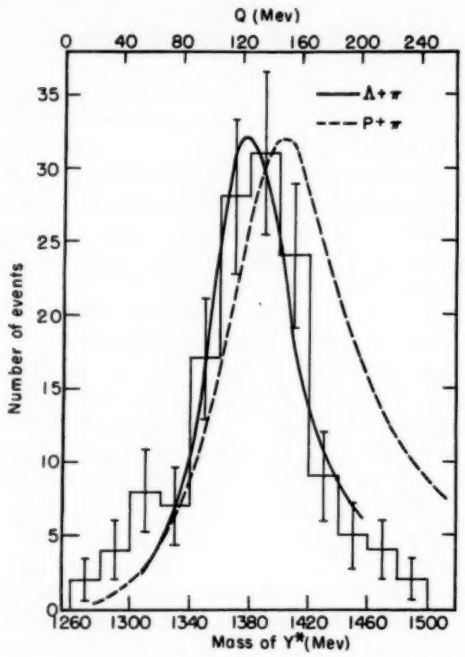

FIG. 2. Mass distribution for Y^* and fitted curves for $\pi\Lambda$ and πp resonances. The lower scale refers only to the $\pi\Lambda$ resonance. Q is the kinetic energy released when either isobar dissociates. The curve for the $\pi\Lambda$ resonances is fitted to the center eight histogram intervals of our data. The πp curve is the fit obtained by Gell-Mann and Watson,[7] to πp scattering data. Both fits are to the formula $\sigma \propto \lambda^2\Gamma^2/[(E-E_0)^2+\frac{1}{4}\Gamma^2]$, where $\Gamma = 2b(a/\lambda)^3/[1+(a/\lambda)^2]$.

tions of the isotopic-spin zero and one amplitudes for the two cases.

The following two methods were used in an effort to determine the spin of Y^*.

(a) The angular momentum of Y^* was investigated by means of an Adair analysis.[5] We first restricted ourselves to production angles with $|\cos\theta| \geq 0.8$. For this angular range the Adair analysis should be valid if only S and P waves are present in the production process. We then computed η for each event, where

$$\eta = \vec{P}_{K^-} \cdot \vec{P}_{\Lambda} / (|\vec{P}_{K^-}||\vec{P}_{\Lambda}|).$$

Of the 29 events with $|\cos\theta| \geq 0.8$, the fraction 0.62 ± 0.09 has $|\eta| \geq 0.5$. If the above-mentioned restriction on the angular interval is sufficient to insure the validity of the Adair analysis, this ratio is expected to be 0.50 for $j = 1/2$ and 0.73 for $j = 3/2$. The experimental result is thus ~1.3 standard deviations from both possibilities, and no conclusion may be drawn from the data. Similar results were obtained for several larger values of the cutoff angle. Presence of D waves, however, cannot be excluded by the production angular distributions (Fig. 3). If they are present, indeed, then none of these choices of angle would be sufficiently restrictive to guarantee the success of the Adair analysis.

(b) Since Y^* may be polarized perpendicular to its plane of production, correlations can exist between the decay angle of the Y^* and the polarization of the resulting Λ. Also, a net Λ polarization

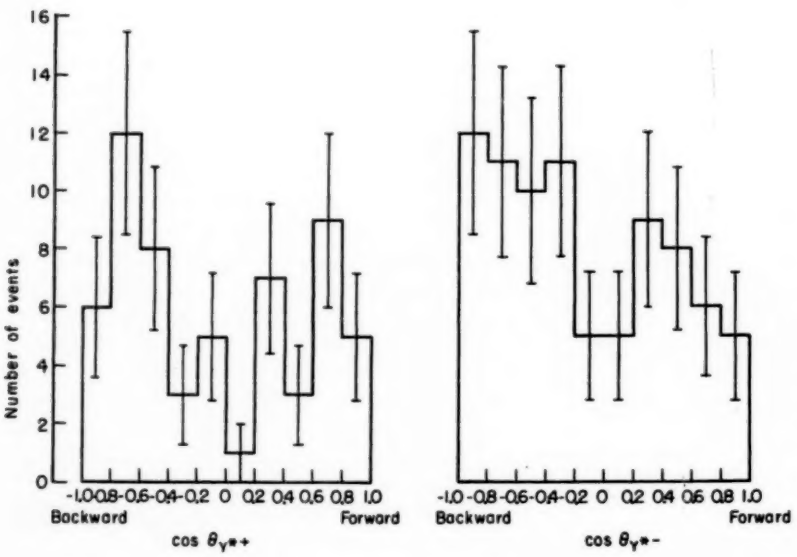

FIG. 3. Angular distribution of $Y^{*\pm}$ in the K^-p barycentric system for the reactions $K^- + p \rightarrow Y^{*\pm} + \pi^{\mp}$.

can result. With our limited data, we see no statistically significant Λ polarization or angular correlations.

However, one can also look for anisotropy, i.e., a polar-to-equatorial ratio, in the decay angle of Y^* with respect to the normal to the plane of production. For spin 3/2, the distribution must be of the form $A + B\xi^2$ by the Sachs-Eisler theorem,[6] independent of the Y^* parity, where we have

$$\xi = (\vec{P}_{K^-} \times \vec{P}_{Y^*}) \cdot \vec{P}_{\Lambda} / (|\vec{P}_{K^-} \times \vec{P}_{Y^*}||\vec{P}_{\Lambda}|),$$

and $\vec{P}_a$ is the momentum of the particle a in the $K^- p$ barycentric system.

Since the coefficient B is a function of the production angle, we want to restrict ourselves to that range of the solid angle where the polar-to-equatorial anisotropy is probably greatest along the normal to the production plane. For production angles near 0 deg and 180 deg (Adair-analysis region), one expects the polar-to-equatorial ratio to be most different from unity in another direction (namely along the direction of the beam). Thus the equatorial region of production angles is more likely to show a large anisotropy along the direction in question. Therefore the production-angle range $\sin\theta \geq 0.866$ was selected for study. We find the ratio of events with $|\xi| > 0.5$ to all events is 0.355. If the distribution is isotropic, as is required for spin 1/2, we expect 0.500 ± 0.063 for our 62 events. The result is thus 2.3 standard deviations from isotropy. The 45-to-1 odds against isotropy overstate the case for higher spin because this is the fourth anisotropy looked for.

Since Y^* may be regarded as a hyperon isobar, which decays into a π and a Λ, it evidently corresponds to a resonance in pion-hyperon scattering. The mass distribution of Fig. 2 then invites a comparison to the cross section for pion-nucleon scattering in the 3/2 - 3/2 state. For this purpose a p-wave resonance formula employed by Gell-Mann and Watson[7] for pion-nucleon scattering was fitted to our $\pi\Lambda$ data by using the eight central histogram intervals of Fig. 2. In fitting the curve, it was found that the interaction radius (a) could be varied over a wide range without changing the goodness of fit appreciably, provided that the reduced width (b) was also changed appropriately. The radius parameter was therefore fixed arbitrarily at $\hbar/m_\pi c$. Table II summarizes our results for Y^*, along with those of Gell-Mann and Watson for the 3-3 resonance.

Even if Y^* does turn out to be a p-wave resonance, there are still many reasons why the π - Λ resonance parameters must not be taken too literally: (a) There is a small contamination of $\Sigma^0\pi\pi$ events in our data. (b) A nonresonant background may be present. (c) The production matrix element for reaction (2) might well depend on the outgoing momentum, and hence distort the mass distribution of Y^*. (d) Two thresholds for other possible decay modes of Y^* appear within the mass interval covered by the resonance curve; i.e., the $\Sigma\pi$ mode threshold around 1330 Mev and the $\bar{K}N$ threshold around 1435 Mev. This must have some effect on the shape of the mass spectrum as observed via the $\Lambda\pi$ decay mode. (e) Final-state pion-pion interaction could disturb the spectrum. (f) Even when the two resonances, Y^{*+} and Y^{*-}, are well resolved in terms of intensity—as in our experiment—there can still be an appreciable interference between the amplitude in which the π^+ arises from reaction (2) and the π^- from reaction (3) and the amplitude in which the roles of the two pions are reversed.

Table II. Parameters for $\pi - \Lambda$ and $\pi - p$ resonance fitted to $\sigma \propto \lambda^2\Gamma^2/[(E-E_0)^2 + \frac{1}{4}\Gamma^2]$, where $\Gamma = 2b(a/\lambda)^3/[1+(a/\lambda)^2]$.

Parameter	$\pi - p$	$\pi - \Lambda$
Interaction radius a in units of $\hbar/m_\pi c$	0.88	1
Reduced width b (Mev)	58	33.4
Resonance energy E_0 (Mev)	159	129.3
Full width at half maximum (Mev)	100	64
Lifetime (sec)		$\sim 10^{-23}$

If we bear all these uncertainties in mind, the resemblance to the 3-3 resonance is certainly remarkable (Fig. 2). The resonance energies when expressed in terms of barycentric kinetic energies differ by only 30 Mev, which is much less than the width of either resonance. Furthermore, the widths are at least comparable.

These results are strongly reminiscent of the concept of global symmetry which predicts two spin 3/2 pion-hyperon resonances, one with $T = 1$, the other with $T = 2$.[8] These are the hyperon counterparts of the $J = T = 3/2$ resonance of the pion-nucleon system. On the other hand, the possibility that Y^* is a $J = 1/2$ resonance cannot be excluded on the basis of our data. The concept of pion-hyperon resonance in either $J = 1/2$ or 3/2 state has been discussed recently by several authors.[9]

A study of $\Sigma^{\mp}\pi^{\pm}\pi^{0}$ events in our experiment is under way at present. The results, however, are too incomplete for us to be able to draw any definite conclusions.

The authors are greatly indebted to the bubble chamber crew under the direction of James D. Gow for their fine job in operating the chamber, especially Robert D. Watt and Glen J. Eckman for their invaluable help with the velocity spectrometers. We also gratefully acknowledge the cooperation of Dr. Edward J. Lofgren and the Bevatron crew, as well as the skilled work and cooperation of our scanning and measuring staff. Special thanks are due the many colleagues in our group who developed the PANG and KICK computer programs—especially Dr. Arthur H. Rosenfeld, and to Dr. Frank Solmitz for many helpful discussions.

One of us (P.E.) is grateful to the Philippe's Foundation Inc. and to the Commisariat à l'Energie Atomique for a fellowship.

[1]Margaret Alston, L. W. Alvarez, P. Eberhard, M. L. Good, W. Graziano, H. K. Ticho, and S. Wojcicki, paper presented at the Tenth Annual Rochester Conference on High-Energy Nuclear Physics, 1960 (to be published).

[2]P. Eberhard, M. L. Good, and H. K. Ticho, Lawrence Radiation Laboratory Report UCRL-8878 Rev, December, 1959 (unpublished); also Rev. Sci. Instr. (to be published).

[3]L. W. Alvarez, P. Eberhard, M. L. Good, W. Graziano, H. K. Ticho, and S. Wojcicki, Phys. Rev. Letters 2, 215 (1959).

[4]L. W. Alvarez, in Proceedings of the 1959 International Conference on High-Energy Physics at Kiev (unpublished); also Lawrence Radiation Laboratory Report UCRL-9354, August, 1960 (unpublished).

[5]R. K. Adair, Phys. Rev. 100, 1540 (1955).

[6]E. Eisler and R. G. Sachs, Phys. Rev. 72, 680 (1947).

[7]M. Gell-Mann and K. Watson, Annual Review of Nuclear Science (Annual Reviews, Inc., Palo Alto, California, 1954), Vol. 4.

[8]M. Gell-Mann, Phys. Rev. 106, 1297 (1957).

[9]R. H. Capps, Phys. Rev. 119, 1753 (1960); R. H. Capps and M. Nauenberg, Phys. Rev. 118, 593 (1960); R. H. Dalitz and S. F. Tuan, Ann. Phys. 10, 307 (1960); M. Nauenberg, Phys. Rev. Letters 2, 351 (1959); A. Komatsuzawa, R. Sugano, and Y. Nogami, Progr. Theoret. Phys. (Kyoto) 21, 151 (1959); Y. Nogami, Progr. Theoret. Phys. (Kyoto) 22, 25 (1959); D. Amati, A. Stanghellini, and B. Vitale, Nuovo cimento 13, 1143 (1959); L. F. Landovitz and B. Margolis, Phys. Rev. Letters 2, 318 (1959); M. H. Ross and C. L. Shaw, Ann. Phys. (to be published).

*This work was done under the auspices of the U. S. Atomic Energy Commission.

†Presently at Laboratoire de Physique Atomique, College de France, Paris, France.

‡ Presently at University of Wisconsin, Madison, Wisconsin.

‖ Presently at University of California at Los Angeles, Los Angeles, California.

SOME CONSIDERATIONS ON THE RECENTLY FOUND EVIDENCE FOR A $\pi\Lambda$ RESONANCE

D. Amati and B. Vitale
CERN, Geneva, Switzerland

and

A. Stanghellini
Istituto di Fisica dell'Università, Bologna, Italy and Istituto Nazionale di Fisica Nucleare, Sezione di Bologna, Italy

(Received November 7, 1960)

Some interest in the possible existence of resonant states in the pion-hyperon system has been raised of late by the analysis of the pion spectra in the reaction $K^{-}+p\rightarrow\Lambda+\pi^{+}+\pi^{-}$.[1] The experimental data fit indeed a phenomenological picture where about 75% of the π^{+} in the previous reaction are produced together with a resonant $\pi\Lambda$ state, whose Q value is peaked at about 115 Mev and whose half-width is ~30 Mev. A detailed analysis of such a resonant state is still missing and many of its characteristics (like its total and orbital angular momentum and the branching ratios in decay) are as yet unknown. It is, however, clear that the very presence of a resonant pion-hyperon state is of importance, as it will help in a deeper understanding of the processes among strongly interacting particles.[2]

On the other hand, the existence of this resonance can give us more confidence in the validity of some theoretical models for the investigation of the pion-hyperon interaction. This was indeed the case with the one-pion approximation static model of Chew and Low for pion-nucleon scattering. As a matter of fact the subsequent dispersive

approach made us understand in a clearer way the fact that just the large 3-3 resonance, by enhancing the one-pion intermediate state, makes the other contributions relatively less important in low-energy pion-nucleon physics.

An analogous model for pion-hyperon interaction was studied some time ago for the case of equal Λ and Σ parities;[3] it is the purpose of this Letter to examine again its results and predictions in the light of the present evidence for the $\pi\Lambda$ resonance. In our case the presence of possible $\bar{K}N$ intermediate states does not make the one-meson approximation unreliable, as the mass of the $\bar{K}N$ states is higher than that of the $\Lambda\pi\pi$ states, and besides no enhancement or resonance is known in low-energy $\bar{K}N$ scattering.

The results of our model, in which the mass difference between Λ and Σ is taken into account explicitly, depend on three parameters: the two normalized pion-hyperon coupling constants, f_Λ and f_Σ, and a parameter Ω which is related to the cutoff energy. The binding energy of Λ in nuclear matter seems to indicate that f_Λ is of the order of the pion-nucleon coupling constant; nothing more can be said at present about the numerical values of f_Λ and f_Σ. We shall discuss in what follows the predictions of our model for values of

$$\delta=(f_\Lambda^2-f_\Sigma^2)/(f_\Lambda^2+f_\Sigma^2) \tag{1}$$

smaller than, let us say, ~ 0.3 (which means $0.5f_\Sigma^2 \leq f_\Lambda^2 \leq 2f_\Sigma^2$). At the end we shall briefly indicate what conclusions can be obtained when more extreme relations between the two coupling constants are assumed.

With the limitation of δ just mentioned, our model predicts two resonant states for $J=3/2$, with $T=1$ and $T=2$, respectively; no resonance can appear either in the $J=3/2$, $T=0$ or in the $J=1/2$ states. The total resonant energies are given by

$$E_\gamma^{\,1}=m_\Lambda+\Omega-\tfrac{1}{2}\Delta-\tfrac{3}{8}\delta\Delta,$$
$$E_\gamma^{\,2}=m_\Lambda+\Omega+\tfrac{3}{2}\Delta+\tfrac{1}{2}\delta\Delta, \tag{2}$$

where $\Delta=m_\Sigma-m_\Lambda=80$ Mev.

It is also possible to predict the half-width of the two resonances, which turns out to be

$$\Gamma_1=\tfrac{4}{3}f_Y^{\,2}\bar{q}^3\,0.72(1+0.66\delta),$$
$$\Gamma_2=\tfrac{4}{3}f_Y^{\,2}q^3(1+0.15\delta), \tag{3}$$

where

$$f_Y^{\,2}=\tfrac{1}{2}(f_\Lambda^{\,2}+f_\Sigma^{\,2}), \tag{4}$$

and $\bar{q}$ and q are the pion momenta in the $\pi\Lambda$ ($T=1$) resonance and in the $\pi\Sigma$ ($T=2$) resonance, respectively.

As the $T=1$ resonance is present both in the $\pi\Lambda$ and in the $\pi\Sigma$ channel, from formulas (12) in I, we can also calculate the branching ratio R for the decay of the resonant state Y^* into either a $\pi\Lambda$ or $\pi\Sigma$ state. As is expected for a narrow resonance, R turns out to be nearly independent of the way the resonance was prepared, which means that

$$\langle\pi\Sigma\,|\,\pi\Sigma\rangle_{T=1}/\langle\pi\Sigma\,|\,\pi\Lambda\rangle\simeq\langle\pi\Lambda\,|\,\pi\Sigma\rangle/\langle\pi\Lambda\,|\,\pi\Lambda\rangle \tag{5}$$

at resonance. We obtain indeed

$$R=(Y^*\to\pi\Sigma)/(Y^*\to\pi\Lambda)\sim\tfrac{1}{2}(0.1)/(1+\delta)^2. \tag{6}$$

Let us now briefly discuss the results contained in (2), (3), and (6). We note that no $\delta\Omega$ corrections are present in (2), which makes the corrections to the resonance energies due to δ rather small. It is interesting to note that, should we take $\Omega=290$ Mev (as in the pion-nucleon case, as global symmetry would suggest), we would get $E_\gamma^{\,1}=1365$ Mev, which means a Q value of 110 Mev, in quite good agreement with the experimental value for the $\pi\Lambda$ ($T=1$) resonance. Or putting it differently, we can determine the numerical value of Ω from the experimental position of the $T=1$ resonance and notice that it turns out to be practically coincident with the position of the 3-3 resonance.

Our model predicts a $J=3/2$, $T=2$ ($\pi\Sigma$) resonance at higher energy. The difference $E_\gamma^{\,2}-E_\gamma^{\,1}$ does not depend on Ω, and is given by

$$E_\gamma^{\,2}-E_\gamma^{\,1}=2\Delta+\tfrac{3}{4}\delta\Delta=(160+105\delta)\text{ Mev}. \tag{7}$$

This formula represents a clear-cut prediction of the theory, based only on the assumption of equal Λ-Σ parities and small δ. Therefore, it would be extremely interesting to investigate experimentally the existence and position of a $T=2$ resonance, by studying for instance the processes $K^-+p\to\Sigma^-+\pi^-+\pi^+$ or $\pi^++p\to\Sigma^++\pi^++K^0$ in the Bev region.

As for the widths and the value of R, we note first that in the limited symmetry case (i.e., $\Delta=\delta=0$) one would have simply

$$\Gamma_1=\Gamma_2=\tfrac{4}{3}f_Y^{\,2}q^3, \quad R=\tfrac{1}{2}. \tag{8}$$

In the expressions (4) and (6) we can therefore

recognize the influence of the nonzero value of Δ (besides the q^3 kinematical factors) and the corrections in δ. We see that while E_γ and the relation (5) are practically insensitive to δ, this is not necessarily the case for the Γ.

The value of R given by (6) gives a preference for the resonance to decay into the $\pi\Lambda$ state, which seems in agreement with the experimental results,[1] even if as yet we have no reliable measurement of the branching ratio.

Several results of our model, obtained with positive Λ-Σ relative parity and small δ, are therefore either in agreement with experiment or susceptible to a direct experimental test. A positive check of the predictions of the model would therefore give a good argument in support of the above-mentioned assumptions.

Should f_Λ^2 and f_Σ^2 be widely different, a new set of resonances could develop in our model. If for instance $f_\Sigma^2 \sim 0$ (we feel safer playing with f_Σ^2, since the order of magnitude of f_Λ^2, as already noted, is roughly known), then all three isotopic channels in the $J=3/2$ states would present resonances; the $T=0$ and $T=2$ would coincide at 240 Mev above that for $T=1$. The $J=1/2$, $T=1$ could also resonate at an energy that could be of the same order as that corresponding to the $J=3/2$, $T=0$ or 2 resonance. It is clear that an experimental investigation of the $T=0$ resonance would also be of great interest. A small nonzero value for f_Σ^2 would, however, remove the $J=1/2$ resonance and, less rapidly, the $J=3/2$, $T=0$ resonance. An independent idea of the relative value of f_Λ^2 and f_Σ^2 would therefore be highly desirable. Perhaps a way that in the near future can be experimentally accessible is the pology (extrapolation) procedure applied to the processes $\Sigma N \to \Lambda N$, $\Sigma N \to \Sigma N$ in the energy region of some hundreds of Mev.

In conclusion, the agreement found between one of the results of our model and the experiment is based on the assumption of equal Λ-Σ parity and depends, to a lesser extent, on the assignment of spin 3/2 to the observed resonance (as global symmetry would suggest). Should these assumptions turn out to be not valid, we could only repeat with Fontenelle[4]: "Je ne suis pas si convaincu de notre ignorance par les choses qui sont et dont la raison nous est inconnue, que par celles qui ne sont point et dont nous trouvons la raison."

We are grateful to Dr. J. Prentki, Dr. Y. Yamaguchi, and Dr. Ph. Meyer for their interest in our work and for useful discussions.

---

[1] M. L. Good, Proceedings of the Tenth Annual Rochester Conference on High-Energy Nuclear Physics (to be published).

[2] A detailed analysis of some implications of the pion-hyperon resonance is given by Ph. Meyer, J. Prentki, and Y. Yamaguchi (to be published).

[3] D. Amati, A. Stanghellini, and B. Vitale, Nuovo cimento 13, 1143 (1959); to be referred to in the following as I. A similar model was studied by M. Nauenberg, Phys. Rev. Letters 2, 351 (1959). For the case of opposite Λ and Σ parities, analogous calculations are in progress at CERN. In formula (12') of I, there is a fortuitous omission of D_1^0, which is given by

$$D_1^0 = 1 + 2(5f_\Lambda^2 - f_\Sigma^2)I\omega - 2(f_\Lambda^2 - f_\Sigma^2)I\Delta.$$

[4] Fontenelle, Histoire des Oracles (Paris, 1687).

ABSTRACTS

In this section are printed the abstracts of Articles that have been forwarded to The American Institute of Physics for publication in THE PHYSICAL REVIEW. In quoting information obtained from this section before the appearance of the corresponding Article, reference should be made to "Physical Review (to be published)" rather than to this Journal.

NEUTRON-PRODUCING MECHANISM IN TRANSVERSE PINCHES. V. Josephson, M. H. Dazey, and R. F. Wuerker, Physical Research Laboratory, Space Technology Laboratories, Los Angeles, California (Received September 28, 1960).

Experiments performed on a transverse pinch assembly show that the presence of a longitudinal magnetic field inside of a conducting plasma and in the reverse direction to that of the external pinching field results in the generation of the $m=0$ (sausage) instability mechanism. This instability mechanism can generate high electrical fields which will accelerate deuterons to energies sufficient for neutron production in deuterium plasmas. Subsequent to the blowup of the instability, the plasma-field configuration is such that the accelerated deuterons can continue to circulate in stable orbits until lost by neutron-producing collisions or by diffusion out of the ends of the geometry.

ELECTROMAGNETIC INTERACTION OF A BEAM OF CHARGED PARTICLES WITH PLASMA. Jacob Neufeld and P. H. Doyle,* Health Physics Division, Oak Ridge National Laboratory, Oak Ridge, Tennessee (Received September 30, 1960).

The plasma-beam instability has been studied by Akhiezer and Fainberg under the assumption that $\theta=0$, where θ is the angle formed by the direction of the beam and the direction of the growing wave resulting from the instability. Under these conditions the interaction is electrostatic, i.e., the wave is longitudinal. In this investigation the above assumption is generalized so as to include the case of $\theta\neq 0$ and the effect of electromagnetic interaction. For $\omega\sim\omega_1$, where ω_1 is the Langmuir frequency of the plasma, the interaction is electrostatic for all values of θ and the resulting instability which produces a longitudinal wave increases exponentially in accordance with the term $\exp(3\sqrt{3}\,\omega_0^2 k v_0 \cos\theta/8)^{1/3}$ (where ω_0 is the Langmuir frequency of the beam). For a frequency range below ω_1 the instability is less pronounced. However, this instability is significant, since the interaction is electromagnetic and the "growing wave" resulting from this interaction is characterized by an electric vector having both transverse and longitudinal components. In investigating the above instabilities an assumption was made that the density of the incident beam is small and the results cover all values of θ except those in the immediate neighborhood of $\pi/2$. For θ in the neighborhood of $\pi/2$ the assumption is more general and the results apply to any density of the beam.

*Now at Michigan State University, East Lansing, Michigan.

EIGENVALUES OF DENSITY MATRICES. B. C. Carlson and Joseph M. Keller, Institute for Atomic Research and Department of Physics, Iowa State University, Ames, Iowa (Received September 8, 1960).

For a system of N identical particles in a pure bound state, the density matrices of positive orders p and $N-p$ have the same nonzero eigenvalues with the same multiplicities. If the number of nonzero eigenvalues is finite, these density matrices are unitarily equivalent.

NEUTRON DIFFRACTION STUDY OF KRYPTON IN THE LIQUID STATE. Glen T. Clayton* and LeRoy Heaton, Argonne National Laboratory, Argonne, Illinois (Received September 19, 1960).

The angular distribution of 1.05A neutrons scattered by krypton in the liquid state at temperatures of 117°K, 133°K, 153°K, 183°K, and 210°K is reported. By use of a sample cell fabricated from a single aluminum crystal, it was possible to obtain diffraction patterns up to the critical temperature and pressure. The scattering curves were Fourier-transformed to obtain the radial atomic distribution function at each temperature. The number of nearest neighbors calculated from these distribution functions range from 8.5 at 117°K to 4.0 at 210°K at distances ranging from 4.02 A to 4.20 A, respectively. A comparison of radial distribution functions from

arbitrarily terminated data shows that the ratio of the last zero atomic density position to the first atomic density maximum position is a function of the amount of intensity data transformed. It also indicates that the width of the bowl of the effective potential in liquid krypton is in approximate quantitative agreement with that of the Lennard-Jones 12:6 potential.

*Present address: University of Arkansas, Fayetteville, Arkansas.

NONLINEAR INTERACTION OF AN ELECTROMAGNETIC WAVE WITH A PLASMA LAYER IN THE PRESENCE OF A STATIC MAGNETIC FIELD. I. THEORY OF HARMONIC GENERATION. R. F. Whitmer and E. B. Barrett, Palo Alto Laboratories, General Telephone and Electronics Laboratories, Palo Alto, California (Received September 16, 1960).

The theory of electromagnetic wave propagation through an anisotropic ionized layer, including the effects of the nonlinear terms in the Boltzmann transport equation, is presented. The method of solution of the nonlinear equations involves an expansion of all of the dependent variables in a Fourier series in time. The differential equations describing wave propagation are then solved, for each frequency in the series, for plane wave propagation, including all of the reflections within the plasma layer. A solution in closed form has been obtained, under small signal conditions, for the field at the hth harmonic in the Fourier series. A discussion of the properties of the wave at the second harmonic frequency as a function of the dc magnetic field strength, the electron density, the electron-neutral particle collision frequency, the field strength of the incident wave, and the thickness of the plasma layer is given.

THEORY OF ELECTRON-PHONON INTERACTIONS. G. D. Whitfield,* Department of Physics, Columbia University, New York, New York, and International Business Machines Watson Laboratory, New York, New York (Received August 30, 1960).

The theory of the interaction of electrons and acoustic phonons in nonpolar crystals has been formulated in terms of a new set of basis states, whose wave functions are essentially Bloch functions that deform with the lattice. The major part of the interaction may then be calculated in terms of the strain tensor rather than the displacement of the lattice. A result of the theory is a generalization of the deformation potential theorem.

*Now at Department of Physics, University of Illinois, Urbana, Illinois.

PHYSICAL PROPERTIES OF SEVERAL II - V SEMICONDUCTORS. W. J. Turner, A. S. Fischler, and W. E. Reese, Research Laboratory, International Business Machines Corporation, Poughkeepsie, New York (Received September 26, 1960).

The physical properties of single crystals of the noncubic II - V semiconducting compounds Zn_3As_2, $ZnAs_2$, ZnSb, Cd_3As_2, $CdAs_2$, and CdSb have been investigated. Energy gaps in these materials vary from approximately 0.13 to 1.0 ev. Mobilities at 297°K range from 10 cm^2/volt-sec to 15000 cm^2/volt-sec and increase at low temperature. Resistivity and mobility anisotropy have been investigated in detail for $CdAs_2$. Except for the $A_3^{II} B_2^{V}$ compounds, high optical transmission has been observed from the intrinsic edge to approximately 30 microns.

ROLE OF DOUBLE EXCHANGE IN THE MAGNETIC STRUCTURE OF $Li_xMn_{1-x}Se$. R. R. Heikes, Westinghouse Research Laboratories, Pittsburgh, Pennsylvania, T. R. McGuire and R. J. Happel, U. S. Naval Ordnance Laboratory, White Oak, Silver Spring, Maryland (Received August 22, 1960).

The details of the magnetic behavior of the $Li_xMn_{1-x}Se$ system are attributed to the double-exchange interaction. At low temperatures, the hole which is introduced by the Li^+ is loosely bound to the Li^+ itself. In the region of the Li ion double exchange causes local distortions of the spin system which we refer to as clusters. As the Li concentration is increased ($x = 0.07$) the clusters overlap sufficiently so that a magnetic field will induce an appreciable magnetic moment ($0.5\mu_B$). At temperatures below 45°K a canted spin ordering is suggested as the magnetic model for the $x = 0.07$ composition. Finally, at $x = 0.10$ we find that spontaneous magnetization develops below 110°K. As the temperature is lowered through 70°K the spontaneous moment

disappears and antiferromagnetism is found. It is not inconsistent with the data for $x = 0.10$ that this antiferromagnetic state is a canted spin system with very small canting angle and therefore small magnetic moment. The theory of de Gennes is used in our discussion of the magnetic model.

MAGNETIC STRUCTURE TRANSITIONS IN $Li_xMn_{1-x}Se$. S. J. Pickart, U. S. Naval Ordnance Laboratory, White Oak, Silver Spring, Maryland, and Brookhaven National Laboratory, Upton, New York, R. Nathans, Pennsylvania State University, University Park, Pennsylvania, and Brookhaven National Laboratory, Upton, New York, and G. Shirane, Westinghouse Research Laboratories, Pittsburgh, Pennsylvania (Received August 22, 1960).

The magnetic structures occurring in lithium-substituted manganese selenide ($Li_xMn_{1-x}Se$) have been examined by low-temperature powder neutron diffraction measurements. The composition with $x = 0.05$ retains the fcc ordering of the second kind found in MnSe, the transition temperature being lowered to 83°K. For $x = 0.07$ the same type of ordering sets in at 73°K, but the spin direction changes abruptly as the temperature is lowered through 45°K; furthermore, the superlattice intensities decrease when an external magnetic field is applied along the scattering vector. At $x = 0.10$, the spontaneous moment observed at 77°K by magnetization measurements is shown to be ferromagnetic, again by means of an external field, and a transition is found at 71°K from ferromagnetism to antiferromagnetism with the third kind of ordering. The results are discussed with relation to models containing canted spins and multiple antiferromagnetic axes.

NUCLEAR MAGNETIC RESONANCE IN SUPERCONDUCTING TIN. G. M. Androes and W. D. Knight, Department of Physics, University of California, Berkeley, California (Received September 16, 1960).

The nuclear magnetic resonance is investigated in small particles (~100A diam) of β tin between 1.5 and 4.2°K, and in magnetic fields between 1.2 and 8.8 kilogauss. The critical temperature and critical field are 3.71°K and 25 kilogauss, respectively. The effective penetration depth for the superconducting particles is estimated to be 1500 A. The resonance linewidth is 0.34% of the magnetic field, and it is independent of temperature. With respect to α tin, the nuclear magnetic resonance shift for β tin is 0.77% in the normal state; it approaches 0.59% in the superconductor as $T \to 0$. (The largest known chemical shift is only 0.17%.) The variation with magnetic field is less than 0.03%. One may conclude that the electronic spin susceptibility in the superconducting particles at absolute zero is approximately three quarters of the normal value. The result for 1000A particles, though less accurate, is substantially the same.

ENERGY DISSIPATION AND SECONDARY ELECTRON EMISSION IN SOLIDS. H. Kanter, Westinghouse Research Laboratories, Pittsburgh, Pennsylvania (Received September 23, 1960).

Experimental evidence is presented for the proportionality between secondary electron yield and the energy dissipated by electrons near the surface of a solid. Using measurements of the energy carried away by electrons transmitted and reflected from thin foils of aluminum and carbon, the energy dissipated in an incremental layer at the exit surface was obtained. Simultaneous measurements of the secondary electron yield showed a close proportionality between the number of secondaries produced and the energy dissipation density near the surface independent of the incident electron energy between 1 and 10 kev. By subtracting the contribution of the back-scattered electrons to the yield at the front surface of a thick aluminum target, the yield of secondaries was found to be proportional to the rate of energy loss calculated from the Bohr-Bethe theory over the energy range investigated.

CONTRIBUTION OF BACK-SCATTERED ELECTRONS TO SECONDARY ELECTRON FORMATION. H. Kanter, Westinghouse Research Laboratories, Pittsburgh, Pennsylvania (Received September 23, 1960).

It is shown experimentally that back-scattered electrons emitted from solids under electron bombardment contribute significantly to the observed secondary yield, even for the case of low back-scattering coefficients. Thus, it was found that in Al with a back-scattering coefficient of only 0.14, about 40% of all secondaries are pro-

duced by back-scattered electrons for initial energies from several kev to several tens of kev. The large contribution of back-scattered electrons to secondary formation even for low-atomic-number materials agrees approximately with what one would expect from the larger rate of energy loss and the greater path lengths of the back-scattered electrons in the secondary-electron escape region compared to that of the incoming primaries.

EFFECT OF PRESSURE ON THE MOBILITY OF INTERSTITIAL OXYGEN AND NITROGEN IN VANADIUM. G. W. Tichelaar,* R. V. Coleman, and D. Lazarus, Department of Physics, University of Illinois, Urbana, Illinois (Received September 13, 1960).

Measurements of stress relaxation as a function of hydrostatic pressure up to 9000 kg/cm^2 have been made on a vanadium sample containing approximately 0.1 atomic percent dissolved oxygen and 0.2 atomic percent dissolved nitrogen. In the temperature range 83.0° to 98.0°C, the relaxation time due to dissolved oxygen is found to increase exponentially with pressure, the value at 9000 kg/cm^2 being about 1.7 times the value at 1 kg/cm^2. The pressure dependence of the stress relaxation can be interpreted in terms of an activation volume of 1.7 cm^3/mole which is about equal to the molar volume of the diffusing oxygen atoms. The relaxation times due to the dissolved nitrogen have been measured at 156.8°C and 163.0°C. The values at 9000 kg/cm^2 are about 1.3 times the values at 1 kg/cm^2, the activation volume being about 1.1 cm^3/mole.

*Present address: Philips Research Laboratories, Eindhoven, The Netherlands.

IMPURITY CONDUCTION IN SILICON. R. K. Ray and H. Y. Fan, Purdue University, Lafayette, Indiana (Received September 23, 1960).

Impurity conduction at low temperature was investigated for various p- and n-type silicon samples. Emphasis was placed on the study of samples of low impurity concentration where the conduction is attributed to charge exchange between impurity centers which are partially ionized by some compensating impurity. A new method was used to determine the compensation. Donors were added to p-type samples by heat treatment. From changes in the room temperature resistivity and the Hall coefficient in the deionization range, the added compensation and the original compensation were determined. The measurement of various samples gave the dependence of the activation energy of conduction on impurity concentration and degree of compensation. The activation energy was much larger for the Ga- and Al-doped samples than for the B-doped samples of comparable impurity concentration. However, it was found that the high activation energies may be the result of ion-pairing between gallium or aluminum atoms and the compensating impurity in the sample. The conductivities of the various samples may be correlated by an expression of conductivity which involves the impurity concentration and the radius of impurity wave function. The results are discussed in the light of current theories of impurity conduction.

THEORY OF THE MAGNETIC ANISOTROPY IN $KMnF_3$. J. J. Pearson, Department of Physics, University of Pittsburgh, Pittsburgh, Pennsylvania (Received September 23, 1960).

A theoretical calculation is made of the magnetic anisotropy in the cubic perovskite structure of $KMnF_3$ at room temperature and in its distorted structures at lower temperatures. These distortions are of two types: first, a small tetragonal distortion of the entire crystal; and then, below the antiferromagnetic Néel point, a distortion of the octahedron of fluorine atoms surrounding each manganese. The cubic anisotropy is obtained from a general spin-wave calculation of the zero-point dipole-dipole energy in a cubic antiferromagnet. The result is found to be the same as that for the ferromagnetic case. The anisotropy from the tetragonal distortion is obtained from the change in the classical Lorentz factors. In calculating the effect of the fluorine distortion a generalization is introduced of Kondo's method for obtaining the anisotropic effective spin Hamiltonian produced by overlap and electron transfer between an Mn^{++} ion and its nonmagnetic neighbors. In its present form the method permits the ready calculation of this anisotropy for any symmetry and number of neighbors. Comparison with the microwave resonance and torque measurements of Portis, Teaney, and Heeger reveals the last effect to be the most important and confirms the form of the spin Hamiltonian found here and its approximate magnitude.

EXCHANGE INTEGRAL IN COBALT FROM SPIN WAVE RESONANCE. P. E. Tannenwald and R. Weber, Lincoln Laboratory, Massachusetts Institute of Technology, Lexington, Massachusetts (Received September 28, 1960; revised manuscript received October 17, 1960).

The exchange constant A and exchange integral J, and their temperature dependences, have been measured in cobalt metal films by spin wave resonance. At room temperature $A = 1.30 \times 10^{-6}$ erg/cm^3 and $J = 155k$. J is temperature independent between 4°K and 295°K. Comparison is made with recent data obtained by other experimental methods.

DECAY OF EXCESS CARRIERS IN SEMICONDUCTORS. II. K. C. Nomura and J. S. Blakemore, Honeywell Research Center, Hopkins, Minnesota (Received August 22, 1960).

A physical interpretation is given of the nonlinear differential equations which govern the decay of excess carrier populations through recombination centers. No restrictions are placed on the magnitudes of the excess carrier densities or the center density. Criteria for trapping are presented; with semiconductors for which the trapping level lies in the opposite half of the intrinsic gap from the Fermi level it is shown that trapping can be described as being of either a temporary or permanent nature. The variety of possible modes of decay are illustrated with the aid of numerical solutions and approximate analytic solutions.

EXCESS TUNNEL CURRENT IN SILICON ESAKI JUNCTIONS. A. G. Chynoweth, W. L. Feldmann, and R. A. Logan, Bell Telephone Laboratories, Murray Hill, New Jersey (Received June 6, 1960; revised manuscript received October 20, 1960).

At low forward biases, a high current flows in Esaki junctions due to band-to-band tunnelling. At sufficiently high biases the current flows by normal forward injection. Between these two bias ranges, the current is unexpectedly high and has been called the excess current. A comprehensive experimental study has been made of this excess current in silicon junctions. It is shown that the properties of the excess current observed so far can be accounted for by a mechanism originally suggested by Yajima and Esaki, in which carriers tunnel by way of energy states within the forbidden gap. Based on this model, the following expression for the excess current, I_x, is proposed:

$$I_x \sim D_x \exp\{-(\alpha_x W_1 e^{1/2}/2)[\epsilon - eV_x + 0.6e(V_n + V_p)]\},$$

where D_x is the density of states in the forbidden gap at an energy related to the forward bias, V_x, and the Fermi energies on the n and p sides are V_n and V_p, respectively, e is the electron charge, ϵ is the energy gap, W_1 is the junction width constant, and α_x is a constant containing a reduced effective mass, m_x. This formula describes the observed dependence of I_x on (*i*) D_x, observed by introducing states associated with electron bombardment, (*ii*) ϵ, studied by the temperature variation of the diode characteristics, (*iii*) V_x, verified from semilogarithmic plots of the forward characteristics, and (*iv*) W_1, tested by using junctions of different widths. From these experiments, $m_x = 0.3m_0$ to within a factor of 2.

The origins of the states in the band gap are not known for certain though they are most likely the band edge tails inherent to heavily doped semiconductors. It is probable that the tunnelling via local states model for the excess current in silicon is applicable to excess currents in other materials.

THERMODYNAMIC GREEN'S FUNCTION METHODS IN NEUTRON SCATTERING BY CRYSTALS. Gordon Baym,* Lyman Laboratory of Physics, Harvard University, Cambridge Massachusetts (Received August 5, 1960; revised manuscript received October 27, 1960).

Formulas are derived for the transition probabilities per unit time for both inelastic coherent scattering of neutrons by crystals, and resonant emission of photons and neutrons by nuclei bound in crystals, without making the assumption that the crystal is harmonic. In deriving these transition probabilities, the analytic structure of thermodynamic correlation or Green's functions, considered as functions of complex temperatures and times, is developed and used. In particular a spectral form is found for the phonon Green's function. Only one assumption is made about the crystal, namely that the displacement of the nuclei due to the forces exerted by the neutron in scattering are linear functions of these forces. This leads to an evaluation of the transition probabilities in terms of the exact thermodynamic

displacement autocorrelation function. This evaluation obeys the detailed balancing condition, and Placzek's sum rule. A consequence of this evaluation is that the widths of the "one-phonon" peaks in the neutron scattering are exactly equal to the widths of the corresponding phonon states of the crystal.

*Present address: Institute for Theoretical Physics, Copenhagen, Denmark.

KNIGHT SHIFT IN POTASSIUM. F. J. Milford and W. B. Gager, Battelle Memorial Institute, Columbus, Ohio (Received December 7, 1959; revised manuscript received September 19, 1960).

The K^{39} nuclear magnetic resonance has been observed in metallic potassium and in aqueous solutions of KNO_3 and $K_3Co(CN)_6$. From these observations a Knight shift of $(0.248 \mp 0.005)\%$ has been obtained. Using Pines' value 0.60×10^{-6} for the spin susceptibility gives $P_f = 0.95\ a_0^{-3}$. This is compared with the theoretical values $0.786\ a_0^{-3}$ obtained by Callaway and $0.909\ a_0^{-3}$ obtained by a quantum defect calculation in this paper.

ELECTRON EFFECTIVE MASSES OF InAs AND GaAs AS A FUNCTION OF TEMPERATURE AND DOPING. Manuel Cardona, Laboratories RCA Ltd., Zurich, Switzerland (Received September 19, 1960).

The electron effective masses of several GaAs and InAs samples at room and liquid nitrogen temperatures have been determined from Faraday rotation and infrared reflectivity measurements. An increase in effective mass with increasing carrier concentration has been found in both materials. This increase can be quantitatively interpreted in InAs in terms of the nonparabolic nature of the conduction band. In GaAs the increase in effective mass with doping suggests the existence of another set of conduction band minima above the lowest (000) minimum. The measured temperature variation of the effective mass can be attributed to two mechanisms: the increase in effective mass produced by the spread in the Fermi distribution because of the nonparabolic shape of the band, and the variation in the band structure produced by the thermal expansion of the lattice.

The Faraday rotation due to the interband transitions has been measured in GaAs and InAs. This rotation is counterclockwise along the direction of the radiation and the magnetic field for GaAs and clockwise for InAs. This effect is compared with the corresponding effect in other semiconductors.

DRIFT VELOCITIES OF SLOW ELECTRONS IN HELIUM, NEON, ARGON, HYDROGEN, AND NITROGEN. J. L. Pack and A. V. Phelps, Westinghouse Research Laboratories, Pittsburgh, Pennsylvania (Received August 29, 1960).

The drift velocities of electrons in helium, neon, argon, hydrogen, and nitrogen have been measured for E/p values between 10^{-4} and 10 volts/cm-mm Hg at temperatures between 77°K and 373°K. The data were obtained from measurements of electron transit time in an improved version of the double-shutter tube developed by Bradbury and Nielsen. By applying sufficiently small voltage pulses to the control grids, it was possible to eliminate end effects present in previous experiments. Values of the momentum transfer cross sections for electrons with energies between about 0.003 and 0.05 ev are obtained which are consistent with the measured drift velocities for thermal electrons in helium, argon, hydrogen, and nitrogen. The derived momentum transfer cross section for electrons in helium is found to be independent of electron energy and equal to 5.3×10^{-16} cm^2. The momentum transfer cross sections for argon, hydrogen, and nitrogen vary with electron energy.

APPLICATION OF THE METHOD OF POLARIZED ORBITALS TO THE SCATTERING OF ELECTRONS FROM HYDROGEN. A. Temkin* and J. C. Lamkin, National Bureau of Standards, Washington, D. C. (Received September 14, 1960).

The s-, p-, and d-wave scattering of slow electrons from atomic hydrogen is calculated by the method of polarized orbitals. Utilization of a transformation of Omidvar avoids the iterative procedure of solving the associated integro-differential equations. The s-wave scattering is smaller than that given by the exchange approximation, and the scattering lengths are within the upper bounds found by Rosenberg, Spruch, and O'Malley. The d-wave phase shifts are too small to explain a resonance in the total cross section.

However, they are much larger than those of the exchange or Born approximation, and they give considerable structure to the differential cross-section curves. The p-wave phase shifts are not much increased by the polarization effects.

*Present address: National Aeronautics and Space Administration, Washington, D. C.

COLLISIONS OF ELECTRONS WITH HYDROGEN ATOMS. VI. ANGULAR DISTRIBUTION IN ELASTIC SCATTERING. H. B. Gilbody, R. F. Stebbings, and Wade L. Fite, John Jay Hopkins Laboratory for Pure and Applied Science, General Atomic, San Diego, California (Received September 28, 1960).

The angular distribution of electrons scattered elastically by hydrogen atoms has been determined for electron energies below 10 ev. The elastically scattered electrons arising from the interaction of crossed electron and modulated hydrogen-atom beams were examined over an angular range extending from 30° to 120°. The results are discussed with reference to other recent experimental and theoretical developments.

NUCLEAR MAGNETIC INTERACTIONS IN HYDROGEN FLUORIDE. Milton R. Baker, H. Mark Nelson,* John A. Leavitt,† and Norman F. Ramsey, Harvard University, Cambridge, Massachusetts (Received September 16, 1960).

The radio-frequency spectra corresponding to the reorientation of the proton and fluorine nuclear magnetic moments in hydrogen fluoride (HF) have been observed in fields of 900, 1800, and 3600 gauss by means of the molecular beam resonance method. Details are presented on the design and construction of the new molecular beam apparatus and electron-bombardment detector used in the experiment. The theory of the HF strong-field energy levels is outlined, and the expected proton and fluorine transitions derived for $J=0$, 1, and 2 are tabulated. From the observed resonance shapes, one can deduce the magnitudes of the spin-rotational interactions of the proton and fluorine nuclei, and their spin-spin interaction. These are: $|c_p| = 71 \pm 3$ kc/sec, $|c_F| = 305 \pm 2$ kc/sec, and $d_1 = 57 \pm 2$ kc/sec. The correctness of these parameters was checked by the good agreement between the experimental curves and resonance shapes predicted by Univac programs using these values. The observed fluorine spin-rotational interaction constant is the largest yet observed and corresponds to a rotational magnetic field at the nucleus of 76 gauss per unit rotational quantum number. The implications of the large spin-rotational interaction for relaxation processes in nuclear magnetic resonance experiments are discussed.

*Present address: Brigham Young University, Provo, Utah.

†Present address: University of Arizona, Tucson, Arizona.

PERTURBATION TREATMENT OF HARTREE-FOCK EQUATIONS. Jan Linderberg,* Department of Physics, University of Florida, Gainesville, Florida (Received August 29, 1960).

For atomic configurations ($1s^2$), ($1s^2 2s$), and ($1s^2 2s^2$) perturbation theory has been used to obtain ($1/Z$) expansions for the Hartree-Fock energies.

*On leave from Quantum Chemistry Group, Uppsala University, Uppsala, Sweden.

INVERSE PHOTONUCLEAR REACTIONS $N^{14}(p,\gamma)O^{15}$ AND $N^{15}(p,\gamma)O^{16}$ IN THE REGION OF THE GIANT RESONANCE. S. G. Cohen,* P. S. Fisher,† and E. K. Warburton, Palmer Physical Laboratory, Princeton University, Princeton, New Jersey (Received September 28, 1960).

The 90° yield of γ rays to the O^{15} ground state from the $N^{14}(p,\gamma)O^{15}$ reaction has been measured for proton energies between 12 and 19.5 Mev covering the region of excitation in O^{15} between 18 and 25 Mev. The excitation curve is quite flat (with $d\sigma/d\Omega$ at 90° ≈ 16 $\mu b/4\pi$ sr), and shows little evidence of the giant resonance. The results for O^{15} are compared to those for N^{15} obtained by Jacobs and Stephens by means of the $N^{15}(\gamma,p)C^{14}$ reaction. The 90° yield of γ rays to the O^{16} ground state from the $N^{15}(p,\gamma)O^{16}$ reaction has been measured for proton energies between 10 and 15 Mev, corresponding to O^{16} excitation energies between 21 and 26 Mev. The excitation curve shows two large resonances peaked at 21.8 and 24.7 Mev, with integral total cross sections of about 0.27 Mev-mb each if no background is assumed. The O^{16} results are compared to theo-

retical calculations of Elliott and Flowers and of others.

*On leave from The Hebrew University, Jerusalem, Israel.

†Now at Clarendon Laboratory, Oxford, England.

HALF-LIFE OF O^{14}. D. L. Hendrie and J. B. Gerhart, Department of Physics, University of Washington, Seattle, Washington (Received September 26, 1960).

The half-life of O^{14} has been remeasured and found to be (70.91 ± 0.04) seconds. The corresponding partial half-life for the $0^+ \rightarrow 0^+$ beta transition is found to be (71.34 ± 0.08) seconds. These results are about 1.6% less than reported earlier. The new half-life is combined with the O^{14} endpoint energy as recently determined by Bardin et al. to re-evaluate the Fermi coupling constant for beta decay. From this, the mean life of the μ meson is calculated. The predicted mean life is greater than the observed value by $(3.3 \pm 0.4)\%$ if the radiative corrections of Kinoshita and Sirlin are used, and by $(1.4 \pm 0.4)\%$ if the radiative corrections of Durand et al. are used.

RELATIVE YIELDS OF NEUTRON GROUPS FROM THE $Li^7(p,n)Be^7, Be^{7*}$ REACTIONS. P. R. Bevington, W. W. Rolland,* and H. W. Lewis,† Duke University, Durham, North Carolina (Received September 23, 1960).

The relative yields of the two groups of neutrons from the $Li^7(p,n)Be^7, Be^{7*}$ reaction, leading to the ground state and the 430-kev state of Be^7, have been measured with a time-of-flight system, using pre-acceleration pulsing of the accelerator beam. Data were taken at 30° intervals between 0° and 150° for proton energies high enough to produce (p,n') neutrons above the detection threshold (300 kev). Since the yield of the (p,n) reaction is more highly peaked in the forward direction than that of the (p,n') reaction, the ratio of the (p,n') to (p,n) intensities grows with increasing angle, severely limiting the usefulness of the (p,n) reaction as a neutron source above the (p,n') threshold at back angles. Absolute differential and total cross sections for both groups have been calculated from the data. A comparison with theory for total cross sections and angular distributions suggests the existence of three previously unidentified levels in Be^8. One level, with $J^\pi = 1^-$, near the threshold for the (p,n') reaction, is responsible for the fast rise in the (p,n') total cross section near threshold. A second level, corresponding to an incident proton energy of about 3.0 Mev, does not contribute significantly to the yield of the (p,n') reaction; the data are consistent with an assignment of $J^\pi = 1^+$ and a total width of 1 Mev. The bulk of the total cross-section curve for the (p,n') reaction has been fitted by assuming a 1^+ level corresponding to an incident proton energy of 3.5 Mev, with $\gamma_n^2 \simeq \gamma_p^2$, $\gamma_{n'}^2 \simeq 5\gamma_p^2$, and $\gamma_{p'}^2 \ll \gamma_p^2$.

*Now at Kings College, Bristol, Tennessee.

†Currently on leave at American University of Beirut, Beirut, Lebanon.

ANGULAR DISTRIBUTIONS FOR $C^{13}(d,n)N^{14}$. Richard Zdanis,* George E. Owen, and L. Madansky, Department of Physics, The Johns Hopkins University, Baltimore, Maryland (Received September 2, 1960).

Angular distributions of neutrons corresponding to transitions to the first (2.31-Mev) and second (3.95-Mev) excited states in the reaction $C^{13}(d,n)N^{14}$ have been measured at an incident deuteron energy of 1.3 Mev. A time-of-flight technique utilizing the associated gamma ray as a trigger was employed to separate the various neutron groups. Because the data, particularly for the first excited state transition, exhibited a relatively large intensity in the backward direction, a simple deuteron stripping process is not sufficient to account for the results. An analysis which included the heavy-particle stripping mode was consistent with the data.

*Now at the Department of Physics, Princeton University, Princeton, New Jersey.

RADIATIONS FROM HIGH-ENERGY POSITRONS INCIDENT ON A BERYLLIUM TARGET. C. P. Jupiter, N. E. Hansen, R. E. Shafer, and S. C. Fultz, Lawrence Radiation Laboratory, University of California, Livermore, California (Received September 23, 1960).

The energy spread and yields of nearly monoenergetic photons of various energies produced by the annihilation in flight of relativistic positrons have been experimentally determined using a 6-in. long by 5-in. diam NaI(Tl) crystal

spectrometer. Photon lines with an energy spread of a few percent are reported. Yields of positrons and monoenergetic photons in the energy range from 2 Mev to 14 Mev have been measured. The bremsstrahlung spectra from 8.5-Mev positrons and electrons were compared and the yields and spectral distributions were found to agree within the experimental error.

LITHIUM-INDUCED REACTION YIELDS BELOW 4 Mev. Edwin Norbeck,* School of Physics, University of Minnesota, Minneapolis, Minnesota (Received September 19, 1960).

Thick-target yields of the following reactions were measured by counting the beta-active products: $Li^7(Li^6, 2n)C^{11}$, $Be^9(Li^6, 2n)N^{13}$, $C^{12}(Li^6, n)F^{17}$, $C^{12}(Li^7, n)F^{18}$, $N^{14}(Li^6, He^5)O^{15}$, $N^{14}(Li^6, d)F^{18}$, $N^{14}(Li^7, t)F^{18}$, $O^{16}(Li^6, n)Na^{21}$, $O^{16}(Li^6, He^4)F^{18}$, $F^{19}(Li^6, Li^5)F^{20}$, $Na^{23}(Li^6, Li^5)Na^{24}$. The reactions $F^{19}(Li^6, 2p)Ne^{23}$ and $Na^{23}(Li^7, Li^6)Na^{24}$ had too small a yield to permit accurate measurement. All of the yield curves show a very rapid but smooth increase of yield with energy. Some general rules are given for estimating the yield to be expected for any positive Q lithium beam reaction in the energy range under consideration.

*Now at State University of Iowa, Iowa City, Iowa.

PROTON GROUPS FROM THE $F^{19}(\alpha, p)Ne^{22}$ REACTION AND THE $Ca^{40}(\alpha, p)Sc^{43}$ REACTION. H. J. Martin,* M. B. Sampson, and D. W. Miller, Indiana University, Bloomington, Indiana (Received September 26, 1960).

A CaF_2 target was bombarded with 21.9-Mev alpha particles and the energies of the outgoing protons were measured with a magnetic spectrometer. Proton groups leading to energy levels in Ne^{22} at excitation energies of 0, 1.28, 3.37, 4.52, 5.18, 5.67, 6.41, 6.88, and 7.49 Mev were seen. The ground-state Q value for the $Ca^{40}(\alpha, p)Sc^{43}$ reaction was found to be -3.47 ± 0.030 Mev. Some information about absolute cross sections and angular distributions for the fluorine and calcium reactions is also presented.

*Now on leave at Brookhaven National Laboratory, Upton, New York.

PHOTONUCLEAR STUDIES WITH MONOENERGETIC GAMMA RAYS FROM THERMAL NEUTRON CAPTURE. Robert E. Welsh* and D. J. Donahue, Department of Physics, Pennsylvania State University, University Park, Pennsylvania (Received September 28, 1960).

Monoenergetic γ rays produced when neutrons are captured in various materials have been used to study the following reactions: $Ta^{181}(\gamma, n)Ta^{180m}$ (8.15 hr), $Au^{197}(\gamma, n)Au^{196}$ (5.6 days), $Ho^{165}(\gamma, n)Ho^{164}$ (34 min), $Ag^{107}(\gamma, n)Ag^{106}$ (24 min), and $Nb^{93}(\gamma, n)Nb^{92}$ (10 days). Cross sections for these reactions have been obtained at several discrete energies between 7.5 and 10.8 Mev. Estimates were also made of the thresholds of these reactions. Two of the thresholds so obtained $Ta^{181}(\gamma, n)Ta^{180m}$, $E_t = 7.60 \pm 0.08$ Mev, and $Nb^{93}(\gamma, n)Nb^{92}$, $E_t = 8.99 \pm 0.04$ Mev, have precision comparable with those of previous measurements of the same quantities.

*Present address: Carnegie Institute of Technology, Pittsburgh, Pennsylvania.

THREE-BODY NUCLEAR PROBLEM WITH REPULSIVE CORE FORCES. Carl Werntz, School of Physics, University of Minnesota, Minneapolis, Minnesota (Received August 3, 1960).

A variational calculation of the binding energy of the triton has been carried out using the Gartenhaus potential. The results indicate that this potential leads to an unbound ground state of the three-nucleon system; this result is attributable to the even-parity tensor potential which is relatively large in magnitude compared to the weakly attractive even-parity central potential. Since this property is also a characteristic of the Signell-Marshak potential, it too should lead to an unbound triton.

COMPARISON OF INELASTIC SCATTERING FROM Sm^{152} WITH COULOMB EXCITATION THEORY. E. M. Bernstein and E. Z. Skurnik, Institute for Theoretical Physics, University of Copenhagen, Copenhagen, Denmark (Received September 9, 1960).

In order to check the theory of electric quadrupole Coulomb excitation, accurate measurements have been made of differential cross sections for inelastic scattering from the first excited state of Sm^{152}. Protons, deuterons, and

alpha particles of energies in the region of 4 Mev were used as the bombarding particles. In addition to the angular distribution of inelastically scattered deuterons, measurements were also made with protons at two scattering angles and at a backward angle with deuterons and alpha particles of different incident energies. The data are found to be in excellent agreement with the semiclassical description of the Coulomb excitation process.

DECAY OF $_{68}Er^{161}$ (3.1 hr). H. A. Grench and S. B. Burson, Argonne National Laboratory, Argonne, Illinois (Received July 8, 1960).

Sources of $_{68}Er^{161}$ (3.1 hr) were produced by the $(n, 2n)$ and (γ, n) reactions. A study of the gamma-ray spectrum by means of scintillation coincidence spectrometry indicated 32 gamma rays. All but three of these are fitted into a tentative decay scheme with levels at 0, 211, 585, 826, 945, 1165, 1253, 1315, 1395, 1450, (1604), 1700, and 1830 kev. The data are consistent with a $3/2^-$ spin assignment to the Er ground state and $7/2^-$ and $1/2^+$ assignments to the ground state and 211-kev state of Ho, respectively. The 826-kev level in Ho probably has $5/2^-$ character.

$Al^{27}(n, \alpha)Na^{24}$ CROSS SECTION AS A FUNCTION OF NEUTRON ENERGY. H. W. Schmitt and J. Halperin, Oak Ridge National Laboratory, Oak Ridge, Tennessee (Received September 16, 1960).

The cross section for the $Al^{27}(n, \alpha)Na^{24}$ reaction has been measured as a function of neutron energy in the range $6.1 \leq E_n \leq 8.3$ Mev and at 14.8 Mev. Measurements were made relative to the fission cross section of U^{238}; activation techniques were used to determine the number of $Al^{27}(n, \alpha)$ events. While a number of peaks and valleys appear in the cross section versus energy curve, there is a general increase in cross section with increasing energy consistent with the Coulomb penetrability of the alpha particle.

CHARGE-EXCHANGE SCATTERING OF NEGATIVE PIONS BY HYDROGEN AT 230, 260, 290, 317, AND 371 Mev. John C. Caris, Robert W. Kenney, Victor Perez-Mendez, and Walton A. Perkins, III,* Lawrence Radiation Laboratory, University of California, Berkeley, California (Received August 29, 1960).

The differential cross section for charge-exchange scattering of negative pions by hydrogen has been observed at 230, 260, 290, 317, and 371 Mev. The reaction was observed by detecting one gamma ray from the π^0 decay with a scintillation-counter telescope. A least-squares analysis was performed to fit the observations to the function

$$\frac{d\sigma}{d\omega} = \sum_{l=1}^{5} a_l P_{l-1}(\cos\theta)$$

in the c.m. frame. The best fit to our experimental measurements requires only s- and p-wave scattering. The results (in mb) are:

E(Mev)	a_1	a_2	a_3
230 ± 9	2.50 ± 0.10	1.39 ± 0.15	2.73 ± 0.28
260 ± 7	2.02 ± 0.08	1.75 ± 0.14	2.15 ± 0.22
290 ± 9	1.45 ± 0.06	1.80 ± 0.10	1.89 ± 0.18
317 ± 8	1.40 ± 0.06	1.85 ± 0.10	1.50 ± 0.17
371 ± 9	1.08 ± 0.05	1.63 ± 0.08	1.18 ± 0.12

The least-squares analysis indicates that d-wave scattering is not established in this energy range.

*Now at Lawrence Radiation Laboratory, Livermore, California.

LIFETIME OF THE NEUTRAL PION. V. Glaser, CERN, Geneva, Switzerland, and R. A. Ferrell, University of Maryland, College Park, Maryland and CERN, Geneva, Switzerland (Received September 6, 1960).

As Primakoff has noted, the phenomenological coupling constant of the neutral pion with the electromagnetic field can be investigated by considering the photoproduction of neutral pions in an external Coulomb field. This is the inverse of the usual two-photon decay (one of the photons being provided by the external field). The relationship between the cross section and the free lifetime of the π^0 is derived. Although the total cross section is small, it is found at high energy that the differential cross section is strongly peaked near the forward direction. The peak cross section is proportional to the fourth power of the photon energy. It is this feature which makes possible an experimental determination of the lifetime by the photoproduction method to an accuracy of about ten percent. A minimum photon energy of one

Gev is required to avoid uncertainties in the nuclear form factor. A higher photon energy would be necessary only if the π^0 mean life is greater than 5×10^{-17} sec. The backgrounds to be expected from nuclear photoproduction are estimated and found to be sufficiently small. In particular, the interference between the coherent nuclear π^0 photoproduction and the Primakoff process is not excessive.

RELATIVISTIC FORMULA FOR THE SPIN CORRELATION COEFFICIENT C_{KP}. D. W. L. Sprung, Department of Mathematical Physics, University of Birmingham, Birmingham, England (Received September 27, 1960).

A formula due to Stapp for the spin correlation coefficient in nucleon-nucleon scattering is corrected. Formulas for the other triple scattering and unpolarized incident beam correlation parameters are included. The formulas are applicable when the nonrelativistic scattering matrix formalism of Wolfenstein is used to analyze triple-scattering experiments at higher energies where relativistic effects are not negligible.

The definition of the correlation coefficients in the relativistic case is discussed.

DETERMINATION OF PION-PION SCATTERING AMPLITUDES SATISFYING DISPERSION RELATIONS AND UNITARITY. John W. Moffat, RIAS, Baltimore, Maryland (Received September 2, 1960).

A method is developed for determining the partial-wave scattering amplitude in terms of the unitarity condition and the known branch cuts and poles of the inverse amplitude. The method is applied to the problem of pion-pion scattering and an implicit solution to the pion-pion partial-wave amplitude is derived for any angular momentum state and for both elastic and inelastic scattering. With the aid of this solution the low-energy resonance behavior of the pion-pion scattering system is studied by neglecting all inelastic processes and concentrating on S and P waves. It is found that a P-wave resonance with a position and width required by nucleon electromagnetic structure can be determined in terms of two parameters. An iteration procedure is described that is applicable when the P wave dominates the equations and this procedure determines the contribution of the unphysical cut. The first iteration of the unphysical cut is numerically integrated on the IBM 709, and the results show that the shift of the resonance position due to the unphysical branch cut can be neglected.

BOSON CURRENTS IN THE THEORY OF WEAK INTERACTIONS. W. B. Zeleny* and A. O. Barut, Department of Physics, Syracuse University, Syracuse, New York (Received May 24, 1960).

A possible new method of introducing boson currents into the weak interaction is suggested. The Bose fields are assumed to obey the first order Kemmer equation. In this way, the boson and fermion currents enter the interaction in a symmetric manner. Three coupling constants are introduced according to the degree of isotopic spin and strangeness symmetries of the currents. The interaction so obtained gives rise in a natural way to the $|\Delta T| = \frac{1}{2}$ selection rule and its violation, and also to fast pionic modes and slow leptonic modes of hyperon decay. First order calculations are performed for K_{l3}^{+}, τ, and τ' decays. Calculations of the decay rates yield sufficient information to determine the approximate magnitudes of the effective coupling constants. The first order calculations are at variance with the experimentally uniform distribution of τ events in the Dalitz plot.

*Now at The University of Sydney, Sydney, N.S.W., Australia.

STOCHASTIC DYNAMICS OF QUANTUM MECHANICAL SYSTEMS. E. C. G. Sudarshan, Department of Physics and Astronomy, University of Rochester, Rochester, New York, P. M. Mathews, Department of Physics, University of Madras, Madras, India, and Jayaseetha Rau, Department of Physics, Brandeis University, Waltham, Massachusetts (Received August 15, 1960).

The most general dynamical law for a quantum mechanical system with a finite number of levels is formulated. A fundamental role is played by the so-called "dynamical matrix" whose properties are stated in a sequence of theorems. A necessary and sufficient criterion for distinguishing dynami-

cal matrices corresponding to a Hamiltonian time dependence is formulated. The non-Hamiltonian case is discussed in detail and the application to paramagnetic relaxation is outlined.

SPIN-MOMENTUM CORRELATIONS IN POSITRON-ELECTRON SCATTERING. C. Fronsdal and B. Jaksic, CERN, Geneva, Switzerland (Received September 27, 1960).

The imaginary part of the fourth order Bhabha ($e^+ - e^-$) scattering matrix element interferes with the (real) second order matrix element, to produce a sixth order dependence of the cross section on the spin of one of the particles (after summing over the spins of the other three particles). The process of extracting the imaginary part of the fourth order matrix element is presented in some detail for one of the graphs (vacuum polarization).